LITHOS 434–435 (2022) 106923

Contents lists available at ScienceDirect

LITHOS

journal homepage: www.elsevier.com/locate/lithos

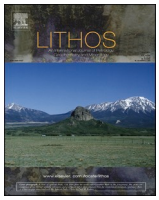

Protolith and metamorphic age of the Sieggraben Eclogites: Implications for the Permian to Cretaceous Wilson cycle in the Austroalpine unit

Ruihong Chang [a], Franz Neubauer [a,d,*], Yongjiang Liu [b,c,**], Johann Genser [a], Sihua Yuan [e], Qianwen Huang [b], Weimin Li [f], Shengyao Yu [b,c]

[a] Paris-Lodron-University of Salzburg, Department of Environment and Biodiversity, Geology Division, Hellbrunnerstraße 34, 5020 Salzburg, Austria
[b] Frontiers Science Center for Deep Ocean Multispheres and Earth System, Key Lab of Submarine Geoscience and Prospecting Techniques, College of Marine Geosciences, Ocean University of China, Qingdao 266100, China
[c] Laboratory for Marine Mineral Resources, Qingdao National Laboratory for Marine Science and Technology, Qingdao 266237, China
[d] State Key Laboratory of Continental Dynamics, Department of Geology, Northwest University, Xi'an 710069, China
[e] China College of Earth Science, Institute of Disaster Prevention, Sanhe, 065201, Hebei Province, China
[f] College of Earth Sciences, Jilin University, Changchun 13006, Jilin Province, China

ARTICLE INFO

Keywords:
Eclogite
Geochronology
Geochemistry
Hf isotopic tracing
Austroalpine unit
Meliata Ocean

ABSTRACT

The Austroalpine eclogite-bearing Sieggraben Complex, exposed at the eastern margin of the Eastern Alps, is considered to represent a subducted and then exhumed fragment of the continental rift, which led to the formation of the Meliata oceanic basin. Combined zircon U-Pb dating, whole rock geochemistry and Hf isotope analysis of the Sieggraben Complex revealed that the eclogite sample shows a protolith age of 242.3 ± 2.6 Ma (Middle Triassic) and displays tholeiitic basalt/N-MORB geochemical characteristics. Associated ultramafic rocks as part of oceanic or subcontinental mantle lithosphere suggest a depleted mantle source and a deep subduction environment. Two zircon grains of eclogites with low Th/U ratios yield ages of 113 ± 2 Ma and 86 ± 4 Ma and represent the approximate age of eclogite metamorphism during Cretaceous. A trondhjemite dike cutting through eclogite gives a crystallization age of 82.19 ± 0.4 Ma and formed by partial melting during decompression. The host metasedimentary rocks are interpreted as old continental crust close to the margin of the Meliata basin were affected by Permian migmatitic metamorphism. The results of this study combined with previous results from the Sieggraben Complex are used to present an updated model for the tectonic evolution of the distal Austroalpine unit associated with the oceanic Meliata relics. The Austroalpine Sieggraben Complex represents a location on the distal continental margin during Permian rifting. This piece of continental crust of an inferred paleotectonic position adjacent to the Meliata oceanic lithosphere subducted during Early Cretaceous times to mantle depth. The subducted continental crust was then exhumed incorporating even ultramafic mantle rocks. During exhumation and decompression of mafic rocks, partial melting took place forming the trondhjemite dike in Late Cretaceous times.

1. Introduction

Continents commonly split along ancient orogens and suture zones, and new oceans are created in between. This re-opening process leads to a new Wilson cycle including rifting, ocean spreading and convergence along roughly the same zones and, consequently, continents re-assembly along similar orogenic zones (Ryan and Dewey, 1997). Subduction represents the most important recycling process, and often includes first subduction of oceanic lithosphere ((B-subduction, B = Benioff-Wadati) followed by subduction of adjacent continental lithosphere (A-subduction, A = Ampferer) both expressed in the occurrence of eclogites and/or blueschists. Often, but not necessarily, between B- and A-subduction

* Correspondence to: F. Neubauer, Paris-Lodron-University of Salzburg, Department of Environment and Biodiversity, Geology Division, Hellbrunnerstraße 34, 5020 Salzburg, Austria.
** Correspondence to: Y. Liu, Frontiers Science Center for Deep Ocean Multispheres and Earth System, Key Lab of Submarine Geoscience and Prospecting Techniques, College of Marine Geosciences, Ocean University of China, Qingdao 266100, China.
E-mail addresses: ruihong.chang@stud.sbg.ac.at (R. Chang), franz.neubauer@plus.ac.at (F. Neubauer), liuyongjiang@ouc.edu.cn (Y. Liu), johann.genser@plus.ac.at (J. Genser), weiminli@jlu.edu.cn (W. Li), yushengyao@ouc.edu.cn (S. Yu).

https://doi.org/10.1016/j.lithos.2022.106923
Received 31 May 2022; Received in revised form 17 October 2022; Accepted 19 October 2022
Available online 26 October 2022

stages, obduction of oceanic lithosphere occurs (Agard, 2021), leaving behind remnants of oceanic lithosphere (ophiolites). The subducted eclogite-bearing complexes provide information on the formation of HP/UHP (high-pressure/ultra-high pressure) rocks in a subduction channel or an accretionary wedge (Agard, 2021). Both mantle rocks and continental and/or oceanic crustal rocks are typical components of exhumed subduction complexes. Therefore, interaction between these rock types records important information on subduction and exhumation processes (Agard, 2021; Hrvanović et al., 2014; Putiš et al., 2018). Furthermore, the mantle rocks of subduction systems often form in the rift or drift (ocean spreading) setting preserving, therefore, information from the initiation and/or early stage of a Wilson cycle (e.g., Manatschal, 2004).

The Alps are the archetype of a continent–continent collisional orogenic belt (Schmid et al., 2004). In particular, the Eastern Alps are the result of the convergence of two independent Alpidic collisional orogenic belts (Froitzheim et al., 2008; Neubauer et al., 2000), the Cretaceous orogenic belt forming the Austroalpine mega-unit superimposed by the Eocene-Oligocene Austroalpine-Stable Europe collision. However, the Austroalpine basement complex represents a thick-skinned fold-and-thrust belt interpreted to comprise the upper continental plate during the Cenozoic collision of the European foreland/Penninic continental crust and the overlying Adriatic microplate (Schmid et al., 2004). The Mesozoic–Cenozoic (Alpidic) tectonic evolution is based on the splitting of the Variscan orogenic belt, including the opening and closure of the Meliata oceanic basin and Piemontais-Ligurian Ocean in two Wilson cycles of orogenic processes (Froitzheim et al., 2008; Neubauer et al., 2000; Putiš et al., 2019). Here, we report, for the first time, the age of protolith formation and the age decompressional melting of eclogites from the poorly investigated Sieggraben Complex. The new results are complemented by dating of detrital zircons of an associated migmatitic paragneiss. Together with data from the literature, the new data help to reconstruct the tectonic evolution of the distal Austroalpine domain adjacent to the Meliata oceanic basin in the Eastern Alps.

2. Tectonic setting

The Austroalpine Sieggraben Complex is located at the eastern margin of the Eastern Alps close to the transition to the Western Carpathians (Fig. 1). The Eastern Alps are the result of two superimposed collisional orogens (Froitzheim et al., 2008; Neubauer et al., 2000). An earlier, Cretaceous orogenic phase evolved within the Austroalpine mega-unit, the latter, Cenozoic phase transported the Austroalpine mega-unit onto Penninic units, which include the Piemontais-Ligurian Ocean relics. The Austroalpine mega-unit represents a thick-skinned basement-cover nappe stack of Cretaceous age, and the late Cretaceous tectonism and eclogite facies metamorphism in the Austroalpine units of the Eastern Alps have been attributed to collisional process resulting from closure of Tethys-related Meliata oceanic basin (Neubauer et al., 2000; Schmid et al., 2004; Froitzheim et al., 2008, Janák et al., 2006, 2015) similar to Western Carpathians (Putiš et al., 2019). The Austroalpine nappe stack was then transported over Penninic units, which include Mesozoic ophiolites and Subpenninic basement units, during the Paleogene (Liu et al., 2001; Schmid et al., 2004). According to the fundamental works by Kozur (1991) and Mandl and Ondreijikova (1991), small relics of the Meliata oceanic basin occur at a high structural level of the Austroalpine mega-unit. Meliata unit relics are mainly exposed in Western Carpathians and Bükk Mts., and in the Florianikogel unit in the Eastern Alps (Fig. 1).

At the eastern margin of Eastern Alps, the Austroalpine nappe stack is composed of, from base to top, the Wechsel, Waldbach and the Kirchberg-Stuhleck nappes, all considered to represent part of the Lower Austroalpine nappes, and of the overlying Sieggraben Complex (Fig. 2).

The Kirchberg-Stuhleck nappe is composed of the Lower Paleozoic Raabalpen Complex (also termed “Grob-Gneiss” unit) and is intruded by the Permian Grobgneiss, a porphyric granite, and rare Permian metagabbros; these units are overlain by Permian-Triassic clastic-carbonatic

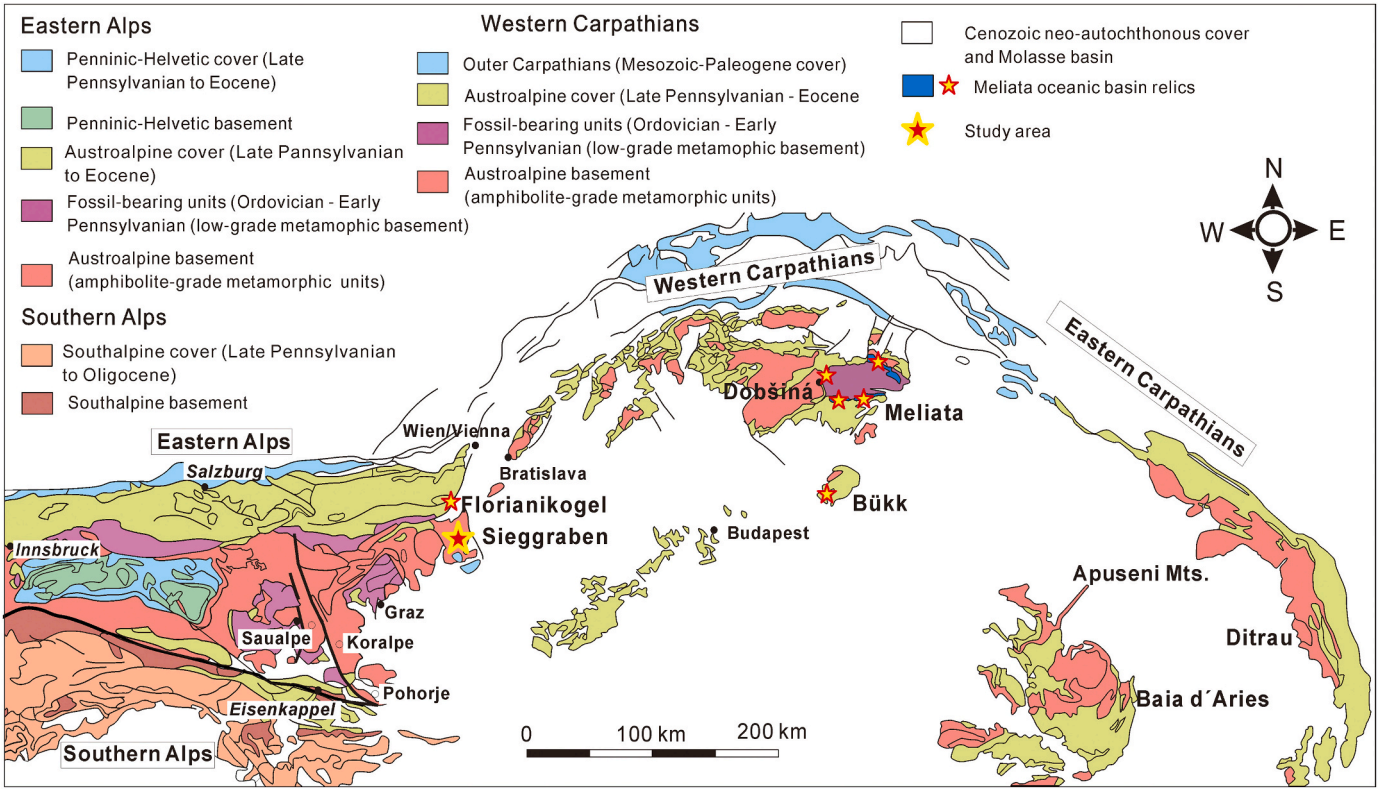

Fig. 1. Overview map of Eastern Alps and Western Carpathians and remnants of the Triassic Meliata oceanic basin.

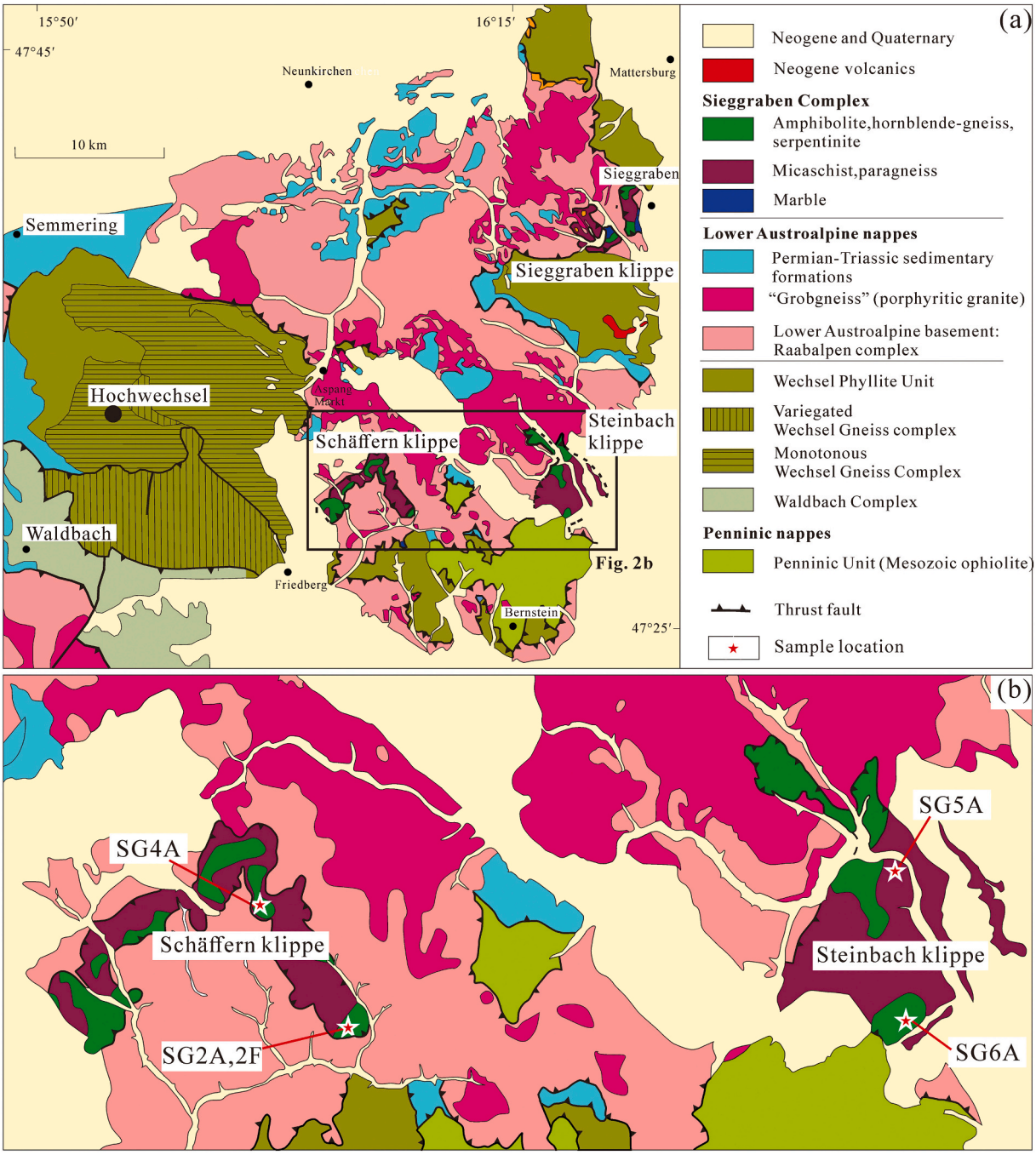

Fig. 2. Geological map of the study area and sample locations (modified after Schnabel, 2002).

cover successions. The Raabalpen Complex was affected by Permian migmatite-grade amphibolite facies metamorphism (Schuster et al., 2001; Yuan et al., 2020) predating the deposition of cover successions. Basement and cover are overprinted by a Late Cretaceous greenschist facies metamorphism (Dallmeyer et al., 1996; Schuster et al., 2001), which locally grades, in the southernmost Raabalpen Complex, into amphibolite facies conditions (Frey et al., 1999). The Sieggraben Complex is overlying the Lower Austroalpine Kirchberg-Stuhleck nappe (Dallmeyer et al., 1996; Neubauer et al., 1999; Putiš et al., 2018) and is considered representing the easternmost extension of the Koriden Complex (in previous literature often also termed Eclogite-Gneiss Unit; Thöni, 2006). At the easternmost Eastern Alps, further south, the Upper Austroalpine Hannersdorf unit is exposed, which comprises a very-low grade metamorphic Silurian-Devonian basement succession of dolomite, slate and greenschists.

The Sieggraben Complex is exposed in three tectonic klippens (Fig. 2a), the Sieggraben, Schäffern and Steinbach klippens, and comprises eclogite and garnet-peridotite, orthogneiss, and marble embedded within partly migmatitic paragneiss (Neubauer et al., 1999; Putiš et al., 2000, 2018) with a Cretaceous high-pressure metamorphism similar to the Koriden Complex (Korikovsky et al., 1998; Miladinova et al., 2021; Neubauer et al., 1999). All lithologic units form a tectonic mélange in which eclogite, carbonate-rich eclogite, amphibolite, and ultramafic rocks occur as meter thick boudins within paragneisses (Fig. 2). Particularly, the garnet-peridotite and other ultramafic rocks (meta-harzburgite and crosscutting meta-pyroxenite dikes) exhibit locally a wide range of petrographic compositions (Hrvanović et al., 2014, 2015; Putiš et al., 2018) and a subcontinental mantle lithosphere Os isotopic

composition of the Steinbach body (Meisel et al., 1997). The eclogite facies P-T conditions were estimated by to 670–750 °C and 1.4–1.5 GPa by Neubauer et al. (1999) for the Schäffern klippe, and, for the Sieggraben klippe, to 1.4–1.7 and 610–750 °C by Putiš et al. (2000) and Kromel et al. (2011) and to 1.7 and 1.9 GPa at 600–650 °C by Miladinova et al. (2021). Neubauer et al. (1999) reported Ar-Ar amphibole ages of 136.1 to 109.5 Ma for the Schäffern klippe, and Dallmeyer et al. (1996) Ar-Ar white mica ages of 78 to 82 Ma from an orthogneiss of the Steinbach klippe and interpreted these ages to date cooling after the eclogite metamorphism. Recently, Miladinova et al. (2021) published a Lu-Hf age of 89.89 ± 0.37 Ma for the Sieggraben klippe eclogite.

The metamorphic assemblages of the Sieggraben unit contrast markedly with the Lower Austroalpine Wechsel and Kirchberg-Stuhleck nappes, which were metamorphosed within greenschist facies of Cretaceous age (Dallmeyer et al., 1996; Frey et al., 1999; Schuster et al., 2001).

3. Samples and petrology

In a small quarry of eclogite (at Zöbersdorf) described by Neubauer et al. (1999 and references therein), unfoliated trondhjemite dikes are cutting through the foliated eclogite (Fig. 3a, b). Except the trondhjemite dikes, contacts between all lithologic elements are penetratively foliated.

Five samples of eclogite and trondhjemite from the abandoned Zöbersdorf quarry in the eastern margin of the Schäffern klippe and ultramafic rocks from the abandoned quarry in the southwestern part of the Steinbach klippe have been collected. In addition, a sample of migmatitic paragneiss was collected from the northern Steinbach klippe. Note that sample numbers (e.g., SG2) also represent the location, and in the case of more than one sample being analyzed from a given location, the samples are given a suffix (e.g., SG2A and SG2F). In the following, the four main types of our samples are described, and details are shown in field photos (Fig. 3a–h) and microphotographs (Fig. 4a–l), particularly the ones used for U-Pb zircon dating. Sample locations and mineralogy are summarized in Table 1.

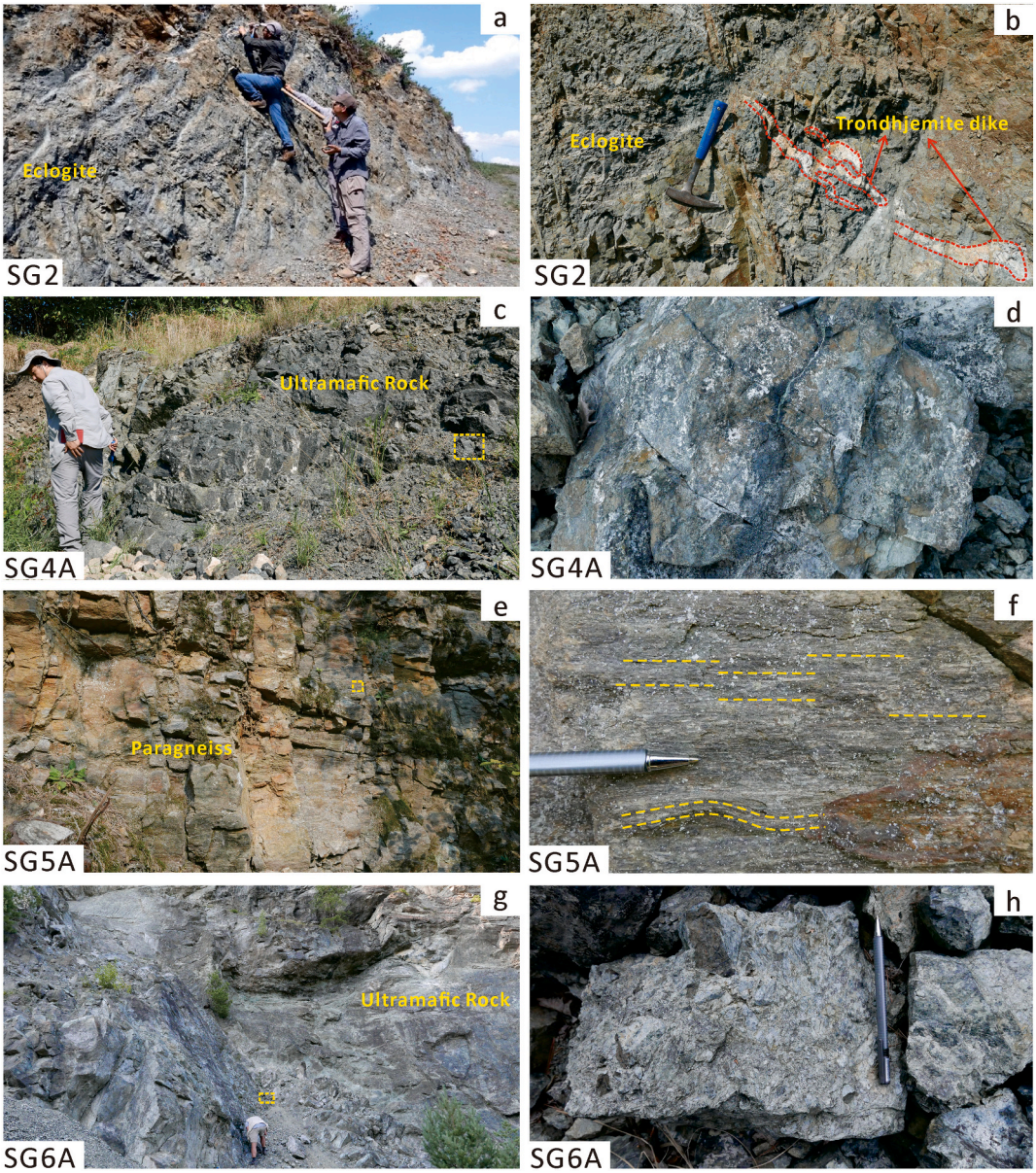

Fig. 3. Field structures and lithologies of the Sieggraben Complex. For description, see text.

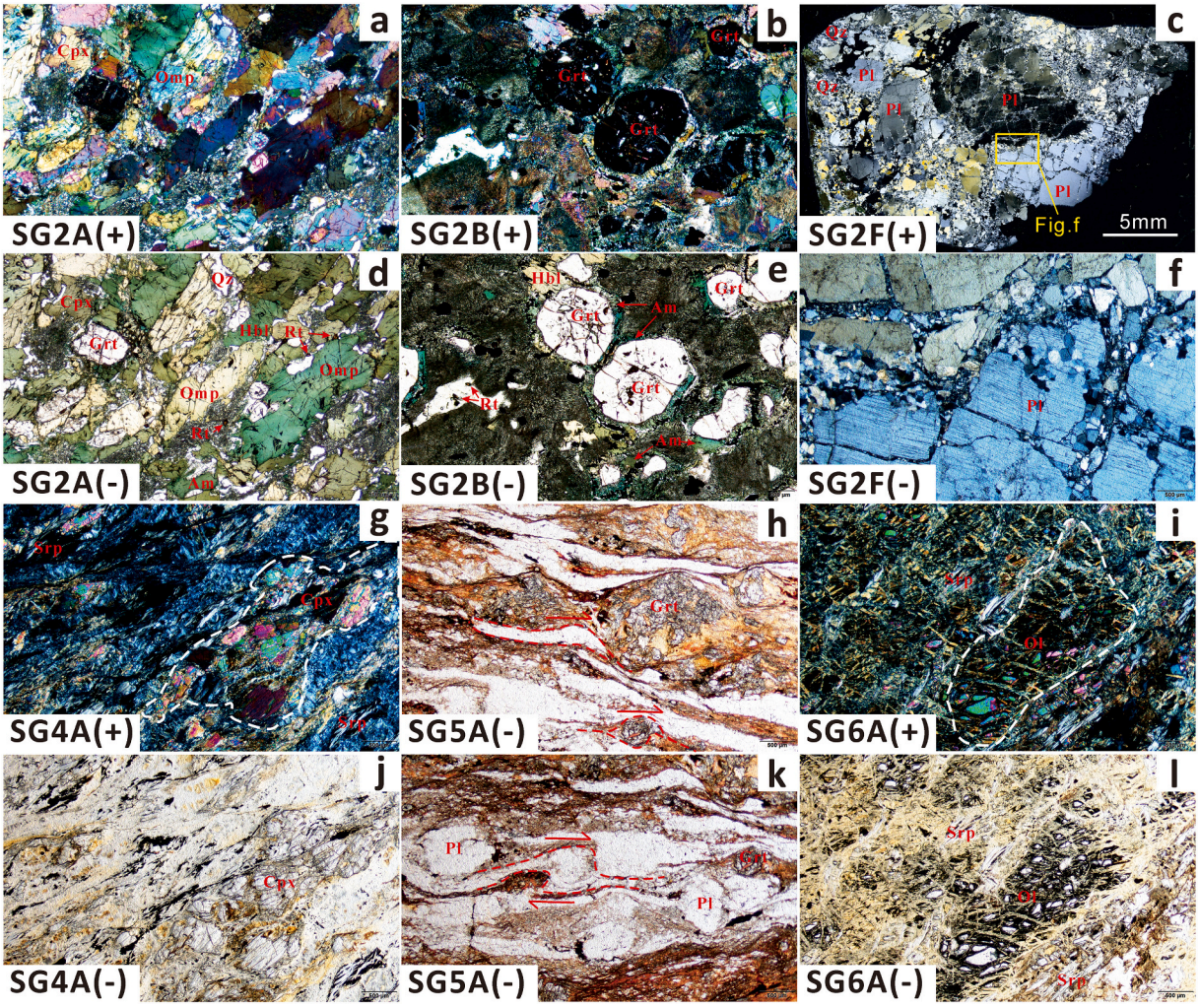

Fig. 4. Microstructures and mineral characteristics of studied samples from the Sieggraben Complex. Notice: (+) means cross-polarized light and (−) means plane-polarized light. For explanation, see text. Abbreviations: Cpx: clinopyroxene, Omp: omphacite, Grt: garnet, Qz: quartz, Pl: plagioclase, Hbl: hornblende, Am: amphibole, Rt: rutile, Srp: serpentine, Ol: olivine.

Table 1
Location, mineralogy and microfabrics of studied samples from the Sieggraben Complex.

Sample	Lithology	Latitude (N)	Longitude (E)	Elevation (m)	Mineralogy	Microfabric
SG2A-E	Coarse-grained eclogite	47°28.366'	16°10.276'	703	Clinopyroxene, omphacite, amphibole, hornblende, garnet, quartz, rutile, zircon	Clinopyroxene replaced by hornblende; elongated omphacite with preferred orientation, amphibole growth around garnet rims
SG4A-F	Serpentinized pyroxenite and peridotite	47°29.634'	16°08.888'	783	Serpentine, clinopyroxene	Serpentinized clinopyroxene, broken to small blocks, coarse-grained clinopyroxene porphyroclasts, serpentinized matrix with mesh structure (after olivine?)
SG6A-F	Serpentinized peridotite	47°28.261'	16°18.463'	426	Serpentine, olivine	Olivine serpentinized, broken to small blocks, serpentine orientated, coarse-grained olivine porphyroclasts; serpentinized matrix with mesh structure
SG2F	Trondhjemite	47°28.366'	16°10.276'	703	Plagioclase, quartz	Fragmentation of plagioclase with many cracks; fine-grained quartz filled between broken plagioclase grains
SG5A	Paragneiss	47°29.978'	16°18.608'	413	Garnet, plagioclase, quartz, biotite	Well developed lineation; shear fabrics, rotated garnet porphyroblasts indicating simple shear

Eclogite (SG2A–E): The eclogites form a several meter thick layer within light-coloured poorly exposed gneisses (Fig. 3a). Sample SG2A is from the margin and SG2B from the center of the eclogite body for studying microfabrics in thin-sections, and SG2A, SG2C–E for geochemical investigations. The eclogites are coarse-grained and bear a weak foliation in the center of the body and are gradually more foliated toward the boundary (Fig. 4a, b) finally changing into fine-grained (0.5–1 mm), mylonitic, retrogressed eclogites. The amphibole content of the eclogite increases from the center to the periphery (Fig. 4d, e). The mineral assemblage contains omphacite, garnet, rutile, and quartz as peak metamorphic assemblage, and diopsidic clinopyroxene and amphibole as retrograde minerals (Fig. 4a–b, d–e). Omphacite grains are elongated (Fig. 4a), replaced by diopsidic clinopyroxene grains and these are replaced again by amphibole during retrogression of the

eclogite (Fig. 4a, d; Neubauer et al., 1999). Amphibole also replaced some of garnet grains forming a rim around garnet grains (Fig. 4d, e).

Trondhjemite (SG2F): The trondhjemite dikes cut through the eclogite body and the eclogite foliation (Fig. 3b). They are porphyritic, internally undeformed, with the mineral assemblage of phenocrystic plagioclase in a fine-grained matrix composed of plagioclase and quartz (Fig. 4c, f). The interior of plagioclase phenocrysts is fragmented and developed many cracks filled by fine-grained quartz (Fig. 4f).

Ultramafic rocks (SG4A, SA6A): Serpentinized ultramafic rocks were investigated from two separate locations (Schäffern and Steinbach klippe) of the Sieggraben Complex (Fig. 3b). Pyroxene and olivine are blocky (Fig. 4d, h) with coarse-grained clinopyroxene and/or olivine porphyroclasts (1–2 cm in size, ca. 35 modal %, Fig. 4g, i) randomly oriented in a fine-grained matrix (approximately 65%) composed of partly serpentinized clinopyroxene and/or olivine with a typical mesh structure (Fig. 4j, l).

Paragneiss (SG5A): A representative migmatitic paragneiss was taken from a major exposure of the Steinbach klippe. In the field, the paragneiss shows a migmatitic appearance with cm-thick lenses of leucosomes (Fig. 3e, f). The paragneiss is strongly foliated and composed of plagioclase, garnet and large amounts of biotite (Fig. 4h, k). Microscopically, deformation with shear fabrics is well developed with a N-S trending stretching lineation and top-N kinematic indicators (Fig. 4k). Garnet and plagioclase porphyroblasts (ca. 0.5–1 cm in size) contain inclusions of quartz, albite, and white mica. The matrix consists of dominantly ca. 0.5 mm large, deformed quartz crystals showing grain boundary migration, as well as plagioclase with subgrains, biotite and opaque ore minerals.

4. Analytical methods

4.1. Zircon geochronology and geochemistry

Zircon grains from eclogite (SG2A), ultramafic rocks (SG4A, SG6A), trondhjemite dike (SG2F) and paragneiss (SG5A) samples were separated for U-Pb dating by conventional heavy liquid and magnetic techniques at the Special Laboratory of the Geological Team of Hebei Province, Langfang, China. Not sufficient zircon grains for successful U-Pb dating were found in ultramafic rocks. Internal structures of zircons were imaged using transmitted- and reflected-light optical microscopy and cathodoluminescence (CL) at the Institute of Geology, Chinese Academy of Geological Sciences, Beijing, China, and then spot positions for dating were selected.

U-Pb dating and trace element analyses of zircons were conducted synchronously by the LA–ICP–MS methodology at the State Key Laboratory of Continental Dynamics of the Northwest University, Xi'an, China. The laser-ablation system used is a GeoLas 200 M equipped with a 193 nm ArF-excimer laser, and a homogenizing and imaging optical system (MicroLas, Göttingen, Germany). Spots were performed on the ELAN 6100 ICP-MS from Perkin Elmer/SCIEX (Canada) with a dynamic reaction cell (DRC). The laser-ablation spot size was set at 32 μm, and laser energy and frequency of 210 mJ and 10 Hz for 40 s were used. Harvard zircon 91500 with a weighted mean $^{206}Pb/^{238}U$ age of 1065.4 ± 0.6 Ma (Wiedenbeck et al., 2004) was used as an external standard and was analyzed twice every 5–10 analyses to correct for both instrumental mass bias and depth-dependent elemental and isotopic fractionation. The NIST610 was used as external reference and internal standard for Si to calibrate the trace element contents. Offline raw data selection and background and time-drift correction of the zircon analysis was performed by the Glitter 4.0 software after $^{207}Pb/^{206}Pb$, $^{206}Pb/^{238}U$, $^{207}Pb/^{235}U$ and $^{208}Pb/^{232}Th$ ratios were calculated. ISOPLOT version 4.15 was used to calculate and plot the U-Pb concordia diagrams and weighted mean ages (Ludwig, 2012).

4.2. Zircon Hf isotopic analysis

Zircon Lu-Hf isotopic analysis was performed on the same zircon grains that were subjected to U-Pb dating by using a Nu Plasma MC-ICP-MS connected to a GeoLas 2005 193 nm laser system. Helium was used as a carrier gas. The spot size was set at 44 μm, while the laser repetition rate was 10 Hz, and the energy density applied was 15–20 J/cm^2. Raw count rates for ^{172}Yb, ^{173}Yb, ^{175}Lu, $^{176}(Hf + Yb + Lu)$, ^{177}Hf, ^{178}Hf, ^{179}Hf and ^{180}Hf were collected simultaneously. The detailed analytical methodology followed that of Yuan et al. (2008). Standard zircons 91500 (Wiedenbeck et al., 1995) and GJ-1 (Jackson et al., 2004) were re-analyzed as an unknown sample to check the quality of the data during the analysis. The obtained $^{176}Hf/^{177}Hf$ ratios of the 91500 and GJ-1 standards were 0.282295 ± 0.000022 (n = 5, 2σ) and 0.282029 ±0.000016 (n = 5, 2σ), respectively, which are in good agreement with the recommended $^{176}Hf/^{177}Hf$ ratios within 2σ (0.282307±0.000058, 2σ; 0.282015±0.000019, 2σ) (Griffin et al., 2006).

The initial $^{176}Hf/^{177}Hf$ values are expressed as εHf(t), which is calculated using the decay constant for ^{176}Lu of 1.867×10^{-11} (Scherer et al., 2001; Söderlund et al., 2004) and present-day chondritic ratios of $^{176}Hf/^{177}Hf = 0.282785$ and $^{176}Lu/^{177}Hf = 0.0336$ (Bouvier et al., 2008). Single–stage Hf model ages (T_{DM1}) were calculated relative to a depleted mantle model with present-day $^{176}Hf/^{177}Hf = 0.28325$ and $^{176}Lu/^{177}Hf = 0.0384$ ratios (Griffin et al., 2002). Two-stage Hf model ages (T_{DM2}) were also calculated, using a $^{176}Lu/^{177}Hf$ value of 0.015 for the average continental crust (Griffin et al., 2002).

4.3. Whole-rock geochemical analysis

In addition to the dated samples, we collected further samples for geochemical analysis in each outcrop. These are similar in petrography varying slightly in the amount of main minerals and microfabrics. The major and trace element compositions of seventeen samples from eclogite (SG2A, C–E), ultramafic rock (SG4A–F, SG6B–F), trondhjemite dike (SG2F) and paragneiss (SG5A) of the Sieggraben Complex were generated using the XRF (Rigku RIX 2100) and the ICP-MS (PE6 100 DRC), respectively. All the analyses were performed at the State Key Laboratory of Continental Dynamics, Northwest University, Xi'an, China. All samples were trimmed to remove weathered surfaces before being cleaned with deionized water and crushed to 200 mesh in an agate mill.

For major element analysis, 0.5 g sample powders were mixed with 5.2 g $Li_2B_4O_7$, 0.4 g LiF, 0.3 g NH_4NO_3 and minor LiBr in a platinum pot and melted to a glass disc in a high frequency melting instrument prior to analysis. For trace element analysis, sample powders were digested using a HF + HNO_3 mixture in high-pressure Teflon bombs at 190 °C for 48 h. Analyses of USGS and Chinese national rock standards (BCR-2, GSR-1 and GSR-3) indicate that both analytical precision and accuracy for major elements are generally better than 5%, and for most of the trace elements except for the transition metals, are better than 2% and 10%, respectively. In addition, one sample was selected randomly to be analyzed twice after every ten samples to assess the accuracy.

5. Analytical results

5.1. U-Pb geochronology

For this study, three samples collected from the Sieggraben Complex were chosen for zircon U-Pb dating by LA-ICP-MS, the zircons from the ultramafic rocks were not analyzed because not sufficient grains were found. CL images of representative zircons and age diagrams are shown in Figs. 5–6, and the U-Pb analytical data are listed in Supplementary Table S1. We use the 95–105% limit of concordance although most data are between 98 and 102%. We use the $^{206}Pb/^{238}U$ age for ages <1.0 Ga.

The zircon grains of the eclogite sample SG2A are mostly subhedral to euhedral, few grains are rounded, elongated, prismatic and range in length from 20 to 80 μm and in width from 20 to 40 μm. In CL images,

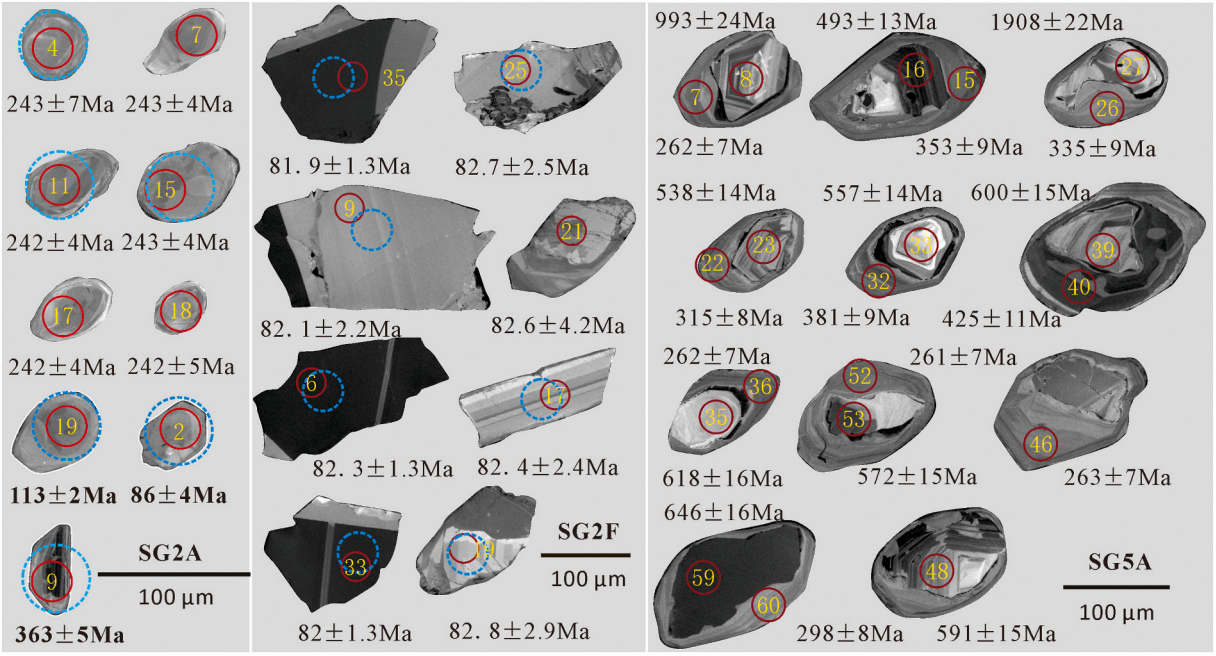

Fig. 5. Cathodoluminescence images of zircons with $^{206}Pb/^{238}U$ ages and/or initial Hf isotope spots for eclogite (SG2A), trondhjemite (SG2F) and paragneiss (SG5A) of the Sieggraben Complex. Red circle shows the location of the U-Pb dating spot, the stippled blue circle the spot used for Hf isotopic tracing. (For interpretation of the references to colour in this figure legend, the reader is referred to the web version of this article.)

most zircon grains exhibit a weak oscillatory zoning (Fig. 5), one grain (no. 9) shows a darker oscillatory zoning. Although the surface of the zircon grains was affected by fluids no influence on the zircon cores was found.

Thirteen U-Pb analyses yield overlapping results on or near the Concordia (Fig. 6) and have low U contents of around 10–300 μg/g and low to intermediate Th/U ratios of 0.14–0.38, with a majority around 0.20 (Supplementary Table S1). Ten of them give the weighted mean $^{206}Pb/^{238}U$ age (242.3 ± 2.6 Ma, MSWD = 0.0119) (Fig. 6). In addition, two spot analyses yield ages of 113 ± 2 Ma (concordant) and 86 ± 4 Ma (slightly discordant) (Figs. 5, 6a), with a Th/U ratio of 0.06–0.08, whereas one zircon spot (no. 9) yields a concordant age of 363 ± 5 Ma (Figs. 5, 6a), which is interpreted as an inherited xenocryst incorporated during magma ascent. In total, at least three distinct zircon growth stages can be resolved (Fig. 5).

Zircon grains of the trondhjemite sample (SG2F) show two groups: One group has angular grains, a dark colour in the CL image, range in length from 150 to 200 μm and in width from 100 to 150 μm, and are characterized by xenomorphic, irregular shapes. CL images also show less structural or intragranular variations of the luminescence. Most grains have no sign of overgrowth or zoning, only one grain exhibits a blurry oscillatory zoning. In the other group, the zircons are finer grained with a length from 100 to 150 μm and a width from 80 to 100 μm. These grains are clear, rounded, subhedral to anhedral, crystals, elongated to prismatic or with well-developed crystal faces. CL images reveal sector zoning in the equidimensional zircon grains and oscillatory zoning in the long prismatic grains. Both groups of zircons show a low CL intensity (Fig. 5).

All the zircons have very low Th/U ratios ranging from 0.0002 to 0.02 and are mostly lower than 0.01 (Supplementary Table S1). Most zircons are concordant and yield a concordia age of 82.42 ± 0.99 Ma (Fig. 6c). Analyses on 25 zircon grains from trondhjemite yield a mean $^{206}Pb/^{238}U$ age of 82.19 ± 0.40 Ma (MSWD = 0.061, n = 25) (Fig. 6d).

Zircon grains of the paragneiss sample SG5A are mostly subhedral to anhedral. Lengths of these grains are about 100 to 150 μm, most are oval to round, multifaceted crystals. CL imaging reveals that most grains have clear core-rim structures (Fig. 5). Many cores reveal oscillatory or sector zonation with a strong luminescence, and these cores are interpreted as detrital zircons. However, the cores are surrounded by strongly recrystallized rims and these rims are therefore younger.

U-Pb analyses on 58 grains are listed in Supplementary Table S1 and are plotted on the concordia diagram (Fig. 6e). Of the subconcordant grains (90–110%), the youngest age is 261 ± 7 Ma (101.5% concordancy), the oldest 2195 ± 21 Ma (Table S1). The age population at 597 ± 8 Ma with subhedral grains often exhibiting an oscillatory zoning represents the majority (Fig. 6f). The mean age of youngest four grains are internally consistent at 262.0 ± 6.9 Ma (Fig. 6e), and these grains are typical magmatic subehedral zircons with an oscillatory zoning (Fig. 5). A concordant grain has a $^{206}Pb/^{238}U$ age of 493 ± 13 Ma (Supplementary Table S1, spot no. 16), whereas most other grains younger than this age have some degree of discordance. The rim ages of three grains range between 315 ± 8 and 381 ± 9 Ma. These rims are homogeneously grey in CL images (Fig. 5) and bear Th/U ratios between 0.01 and 0.14 and represent metamorphic grains.

5.2. Zircon Hf isotopic analysis

Based on U-Pb dating results, representative zircon grains from two samples (SG2A and SG2F) of the Sieggraben Complex were selected for in-situ Hf isotope analysis using LA-MC-ICP-MS. The results are listed in Table 2 and are shown in Fig. 7.

Seven magmatic zircons from the protolith 242 Ma-old eclogites (SG2A) have $^{176}Hf/^{177}Hf$ ratios of 0.283067–0.283174, εHf(t) values of +15.7 to +19.4. Eleven grains from the magmatic 82 Ma-old trondhjemite (SG2F) have $^{176}Hf/^{177}Hf$ ratios of 0.282971–0.283058, εHf(t) values of +8.7 to +11.7, with model ages of 402–591 Ma.

In-situ trace-element analyses of the zircons from the U-Pb dated samples were performed by using LA-ICP-MS. In this study, the analytical procedures were the same as the analyses of U-Pb dating, the results are listed in Supplementary Table S2.

Analyzed REE compositions of the SG2A and SG2F zircons were normalized by CI-chondrite compositions (McDonough and Sun, 1995). REE patterns of zircon grains reveal that they are strongly depleted in light REEs relative to heavy REEs, anomalous behaviours of Ce and Eu in

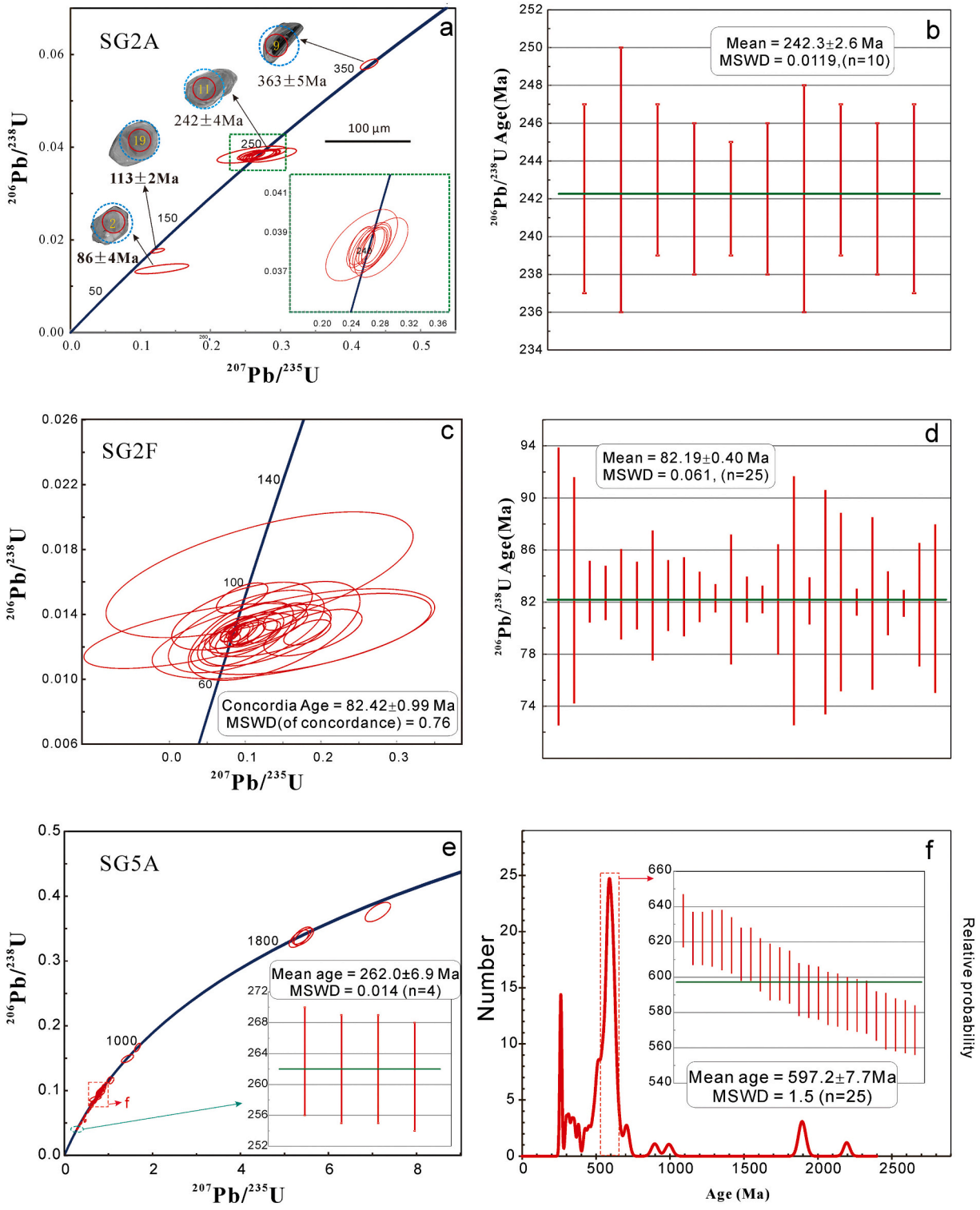

Fig. 6. Zircon U-Pb concordia diagram (a, c, e), $^{206}Pb/^{238}U$ weighted mean age diagrams (b, d insert in e) and the age spectrum diagram (f) for three dated samples from the Sieggraben Complex. The $^{206}Pb/^{238}U$ weighted mean age in (b) is interpreted as the protolith age of the eclogite, and the age in (d) as the age of trondhjemite formation.

chondrite-normalized(CN) patterns are expressed as $Ce/Ce^* = Ce_{CN}/(La_{CN} \times Pr_{CN})^{1/2}$ and $Eu/Eu^* = Eu_{CN}/(Sm_{CN} \times Gd_{CN})^{1/2}$, respectively. The same with sample SG5A, all samples have a pronounced positive Ce anomaly and negative Eu anomaly typical for magmatic zircons (Hoskin and Schaltegger, 2003). The Hf contents in eclogite and trondhjemite range from 8169 to 31,175 μg/g, and Y content from 134 to 152 μg/g. The REE patterns of the eclogite zircon cores overlap with those of the trondhjemite in the Sieggraben Complex (Fig. 7c). Furthermore, as shown in Fig. 7d, the Th/U ratios of zircons (only including zircons with ages younger than 500 Ma from SG5A), especially those in the protolith of eclogite with Triassic ages, have high Th/U values (Fig. 7d).

Table 2
Hf isotopic data of zircons from eclogite of the Siegraben Complex.

Sample No.	Age (Ma)	$^{176}Yb/^{177}Hf$	2σ	$^{176}Lu/^{177}Hf$	2σ	$^{176}Hf/^{177}Hf$	2σ	$e_{Hf}(t)$	$e_{Hf}(t)'$	2σ	T_{DM} (Ma)	T^{C}_{DM} (Ma)	$f_{Lu/Hf}$
SG2A-01	243	0.009409	0.000270	0.000474	0.000015	0.283155	0.000020	18.8	19.5	0.7	134	67	−0.99
SG2A-02	243	0.007462	0.000077	0.000388	0.000004	0.283106	0.000020	17.1	17.8	0.7	203	178	−0.99
SG2A-03	243	0.006401	0.000092	0.000352	0.000006	0.283067	0.000016	15.7	16.3	0.6	257	265	−0.99
SG2A-04	243	0.007585	0.000065	0.000367	0.000004	0.283148	0.000017	18.6	19.2	0.6	144	83	−0.99
SG2A-05	243	0.011935	0.000170	0.000603	0.000010	0.283174	0.000023	19.5	20.3	0.8	108	26	−0.98
SG2A-06	243	0.006105	0.000131	0.000314	0.000008	0.283151	0.000020	18.7	19.4	0.7	139	74	−0.99
SG2A-07	243	0.010640	0.000076	0.000545	0.000003	0.283109	0.000016	17.2	17.7	0.6	200	174	−0.98
SG2F-01	82	0.091329	0.000554	0.004941	0.000025	0.283058	0.000011	11.7	12.1	0.4	307	402	−0.85
SG2F-02	82	0.091001	0.000386	0.004918	0.000008	0.283034	0.000011	10.8	11.2	0.4	345	457	−0.85
SG2F-03	82	0.043987	0.000127	0.002382	0.000004	0.282971	0.000014	8.7	9.2	0.5	414	591	−0.93
SG2F-04	82	0.032235	0.001125	0.001852	0.000070	0.283019	0.000015	10.4	11.0	0.5	338	480	−0.94
SG2F-05	82	0.025916	0.000193	0.001349	0.000010	0.283048	0.000009	11.5	11.8	0.3	291	412	−0.96
SG2F-06	82	0.042195	0.001021	0.002081	0.000056	0.282994	0.000014	9.6	10.0	0.5	376	537	−0.94
SG2F-07	82	0.056949	0.000112	0.003066	0.000003	0.283020	0.000011	10.4	10.8	0.4	349	483	−0.91
SG2F-08	82	0.054610	0.000401	0.002503	0.000011	0.283008	0.000010	10.0	10.4	0.4	360	507	−0.92
SG2F-09	82	0.061468	0.000135	0.002724	0.000001	0.283029	0.000011	10.7	11.1	0.4	331	460	−0.92
SG2F-10	82	0.061850	0.000063	0.002762	0.000003	0.283038	0.000011	11.0	11.4	0.4	318	441	−0.92
SG2F-11	82	0.049078	0.000057	0.002281	0.000002	0.283035	0.000009	11.0	11.3	0.3	318	445	−0.93
SG2F-01	243	0.091329	0.000554	0.004941	0.000025	0.283058	0.000011	14.7	15.1	0.4	307	334	−0.85
SG2F-02	243	0.091001	0.000386	0.004918	0.000008	0.283034	0.000011	13.8	14.2	0.4	345	389	−0.85
SG2F-03	243	0.043987	0.000127	0.002382	0.000004	0.282971	0.000014	12.0	12.5	0.5	414	505	−0.93
SG2F-04	243	0.032235	0.001125	0.001852	0.000070	0.283019	0.000015	13.8	14.3	0.5	338	390	−0.94
SG2F-05	243	0.025916	0.000193	0.001349	0.000010	0.283048	0.000009	14.9	15.2	0.3	291	319	−0.96
SG2F-06	243	0.042195	0.001021	0.002081	0.000056	0.282994	0.000014	12.9	13.4	0.5	376	449	−0.94
SG2F-07	243	0.056949	0.000112	0.003066	0.000003	0.283020	0.000011	13.6	14.0	0.4	349	402	−0.91
SG2F-08	243	0.054610	0.000401	0.002503	0.000011	0.283008	0.000010	13.3	13.7	0.4	360	421	−0.92
SG2F-09	243	0.061468	0.000135	0.002724	0.000001	0.283029	0.000011	14.0	14.4	0.4	331	376	−0.92
SG2F-10	243	0.061850	0.000063	0.002762	0.000003	0.283038	0.000011	14.3	14.7	0.4	318	357	−0.92
SG2F-11	243	0.049078	0.000057	0.002281	0.000002	0.283035	0.000009	14.3	14.6	0.3	318	359	−0.93

5.3. Geochemistry

Four samples of eclogite, eleven samples of ultramafic rocks, one trondhjemite and one paragneiss were collected for whole rock major and trace element analysis. The results are listed in Supplementary Table S3.

On the Zr/Ti versus Nb/Y diagram (Pearce, 1996), most eclogite samples plot within the basalt field (Fig. 8a), and on the Th/Yb vs. Zr/Y (Ross and Bédard, 2009), all samples fall into the tholeiitic (basalt) field (Fig. 8b).

The eclogite samples show SiO_2 contents ranging from 48.75 to 50.13 wt% and LOI- (loss of ignition) (0.93–1.21 wt%) corrected silica contents of 49.42–50.67wt%. These eclogite samples have MgO contents of 6.81–7.35wt% with varying Mg# values of 55.1–59.8. The K_2O contents range from 0.24 to 0.36 wt%, and their total alkalis (K_2O + Na_2O) range from 3.42 to 3.87wt%. They also have variable TiO_2 contents of 0.86–1.01wt%, Al_2O_3 contents of 14.10–15.36wt% and total Fe_2O_3 contents of 11.25–12.96wt%. The rare earth elements of eclogite samples are depleted in light rare earth elements (LREE) (Fig. 9a; Boynton, 1984), with $(La/Lu)_N$ and $(La/Yb)_N$ values of 0.57–0.76 and 0.58–0.85, respectively, both are <1 (Supplementary Table S3). All samples have uniform REE patterns and show a typical N-MORB-like positive slope (Fig. 9a). In the primitive mantle-normalized multi-element variation diagram (Fig. 9b; Sun and McDonough, 1989), based on typical N-MORB (Fig. 9b), eclogites show enrichment in Ba, U, K, Sr and depletion in Th, P and Ti.

In the two studied ultramafic rock types, the high degree of serpentinization is represented by the LOI 8.76–11.91 wt%, we consider LOI-free main elements, they contain SiO_2 44.4–47.2 wt%, high MgO = 35.2–40.7 wt%, and very low Na_2O contents implying little additions of alkalis during serpentinization, high Ni (1444–1970 μg/g) and Mg#s (=100*molar Mg/(Mg + Fe)) (86.6–89.7), low $(La/Lu)_N$ = 0.59–1.01, $(La/Yb)_N$ = 0.69–1.30. Conversely, the REE contents (0.97–4.16 μg/g) of the ultramafic rocks are very low. We collected the data from two ultramafic rock types from Putiš et al. (2018) (Fig. 9, shaded background), which show the depletion in Nb, Zr, Hf, Ti and anomalous behaviour of Eu in one type (pink in Fig. 9), which is similar to our ultramafic rocks. The REE data of show a hump-shaped pattern (Fig. 9a) different from our investigated samples.

The total rare earth element (REE) abundance of the trondhjemite is 5.26 μg/g, like that of ultramafic rocks, and the total REE content of paragneiss is 252 μg/g, with $(La/Lu)_N$ and $(La/Yb)_N$ ratios of 0.89 and 0.90, respectively, both <1 for the trondhjemite. Taken together, the trondhjemite shows similar characteristics as the eclogite. The rock has a clear enrichment of Ba, U, K, Sr, and depletion of Th, Nb and Ti (Fig. 10b), implying a similar trend with eclogite and ultramafic rocks. While the paragneiss shows a continental margin character by its high SiO_2 (71.81 wt%) and K_2O (3.08%) contents and high $(La/Yb)_N$ (52.8) and $(La/Lu)_N$ (45.9) ratios.

6. Discussion

6.1. Geochronology and petrogenesis

6.1.1. Protolith age of eclogite

It is accepted that magmatic and metamorphic zircons can be statistically distinguished by their Th/U ratios (Hoskin and Schaltegger, 2003) although this approach not always applies (e.g., in migmatites, Li et al., 2022) as shown by the dated trondhjemite of this study, too. The Th/U ratios of Triassic zircons of the eclogite in our study are between 0.14 and 0.38, most grains scatter at ca. 0.2 indicating a magmatic origin of these zircons. Furthermore, the rare earth element patterns of eclogitic zircons show positive Ce anomalies and high HREE and Th contents, supporting the magmatic nature of dated zircons (Rubatto, 2017), and whole rock compositions show no Eu anomalies indicating their origin as basaltic liquids. Results of precise LA-ICP-MS zircon U-Pb dating show that the protolith age of the eclogite from Sieggraben Complex is 242.3 ± 2.6 Ma (ca. Anisian/Ladinian boundary). The temperature of eclogite formation in this outcrop (670–750 °C; Neubauer et al., 1999) was not high enough for zircon resetting. The presence of appreciable Sr contents in the eclogite indicates cycling of oceanic Sr and K in the high-pressure fluid (Scambelluri et al., 2001). This age implies that the protolith of the metamorphosed mafic rocks in Sieggraben Complex was formed in Middle Triassic times. This is the

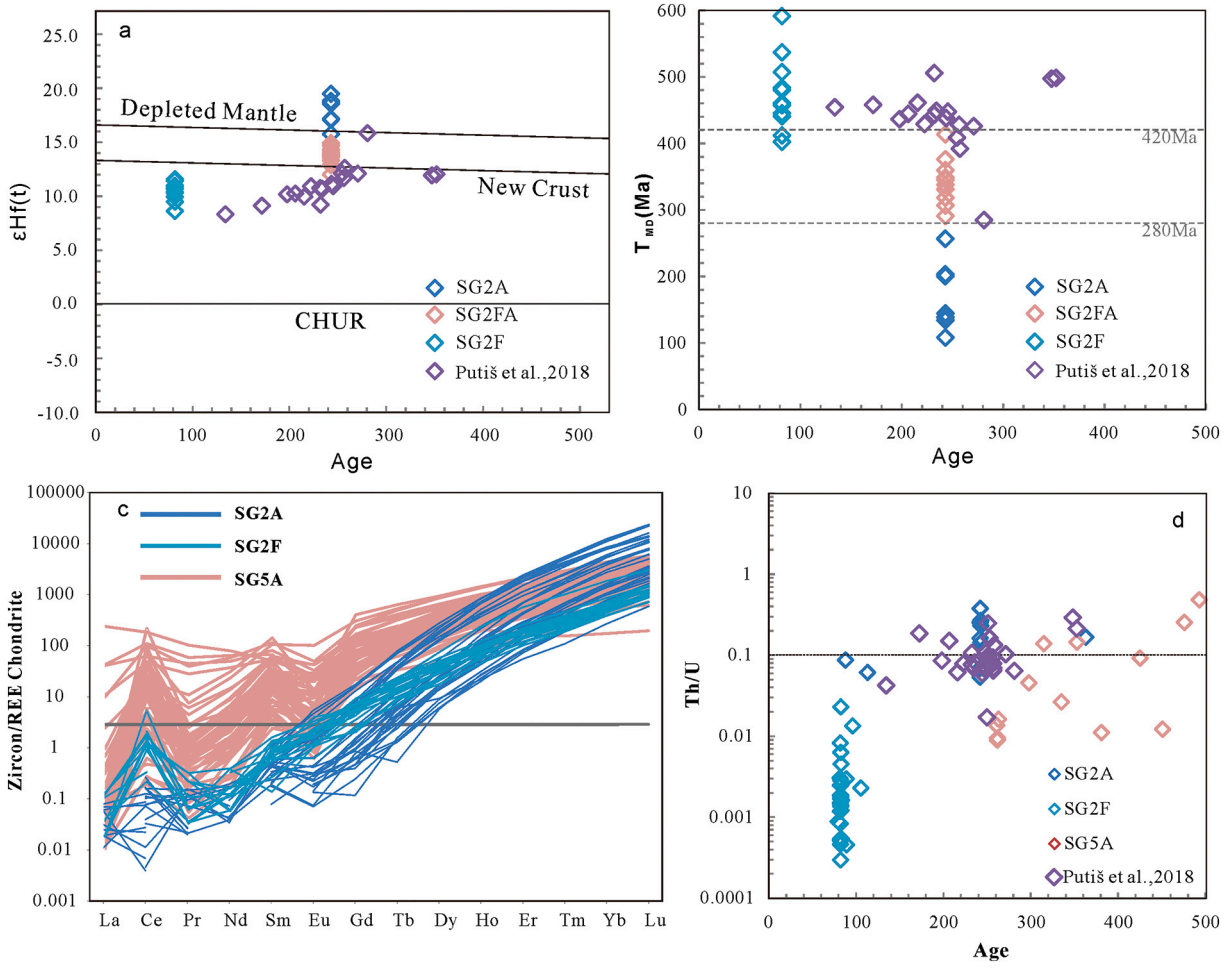

Fig. 7. Plots of eHf(t) vs. U-Pb age (a), $^{176}Hf/^{177}Hf$ versus age of concordant zircons (b), chondrite-normalized REE patterns (c) and age vs. Th/U ratio (d) of zircon grains from eclogite, trondhjemite and paragneiss in the Sieggraben Complex, Eastern Alps. CHUR: Chondritic Uniform Reservoir (Dhuime et al., 2011). CI (chondrite Ivuna) values are from Taylor and McLennan (1985).

first Triassic mafic magmatic rock reported from the Austroalpine nappe complex and is different to the Late Permian age (Sm-Nd, 275 ± 18 Ma, 254.4 ± 8.7 Ma) of eclogitized metagabbros from the Koralpe (Thöni and Jagoutz, 1992). From the geochemical character, we consider that the eclogite and trondhjemite have the same source. Consequently, calculating model age for SG2F with the protolith age of SG2A, a young, Variscan model age results implying juvenile material (SG2FA; Table 2). This corresponds to the inherited zircon age (363 Ma) of the eclogite sample SG2A mentioned above.

Studies have demonstrated that large-ion-lithophile elements (LILE), such as K, Rb, Sr and Ba, as well as U, are mobile during seawater alteration and low-grade metamorphism of ocean floor rocks (e.g., Verma, 1981). However, by comparing the high-grade metamorphic rocks to equivalent igneous rocks, Spandler et al. (2004) have shown that high-pressure metamorphism produce very minor chemical changes, with no significant mobility of high-field strength elements (HFSE), such as Ti, Nb, Ta, Zr, Hf, metals such as, V, Ni, Cr and Fe, and rare earth elements (REE) during subduction-zone metamorphism (e.g., Bienvenu et al., 1990) and serpentinization processes (Scambelluri et al., 2001). Our petrographic work shows that most samples have undergone strong metamorphism and/or some degree of alteration/hydration, mainly affecting the ultramafic rocks. In this study, therefore, only relatively immobile elements are used in the following geochemical discussion. The geochemistry of the studied eclogites is more enriched in Sr, K, U, Ba than normal basalts (Fig. 9b) and depleted in Th, Nb, Ta P and Ti,which are considered to be caused by either crustal contamination or a magma source, which is influenced by the input of subducted material (Sun and McDonough, 1989). We argue that the tholeiitic basalt/N-MORB protoliths of Sieggraben eclogites were emplaced as sills within the middle/lower crust of the rifted continental margin or, less likely, as a part of opening oceanic crust close to the continental margin as found in some magma-poor passive margins (e.g., Whitmarsh et al., 2001). No other member of an ophiolite succession like gabbro or mafic/ultramafic cumulate rocks was found in the Sieggraben Complex making the ophiolitic origin unreasonable. The most plausible explanation is that the studied eclogites represent tholeiitic-basaltic liquids characterized by an evolving magma-rich passive margin similar to undated eclogite protoliths with a similar tholeiitic basaltic signature (Miller et al., 1988, 2007), excluding the dated metagabbros (Thöni and Jagoutz, 1992) with a different chemistry, of the Eclogite-Gneiss Unit of the Koralpe-Saualpe region.

The extremely young Hf isotopic T_{DM} values of the Sieggraben eclogite also suggest that the mafic magmas did not undergo significant contamination by older continental crust during magma ascent. The values above the depleted mantle line in Fig. 7a and b are influenced by high ^{176}Yb. Nb-Ta depletion can be caused by either crustal contamination or a magma source, which is influenced by the input of subducted material (Sun and McDonough, 1989). However, all eclogite zircons have clearly positive εHf(t) values, the extensive crustal contamination can be excluded. Thus, the geochemical and isotopic characteristics of the eclogite are inherited from their mantle source rather than by crustal assimilation.

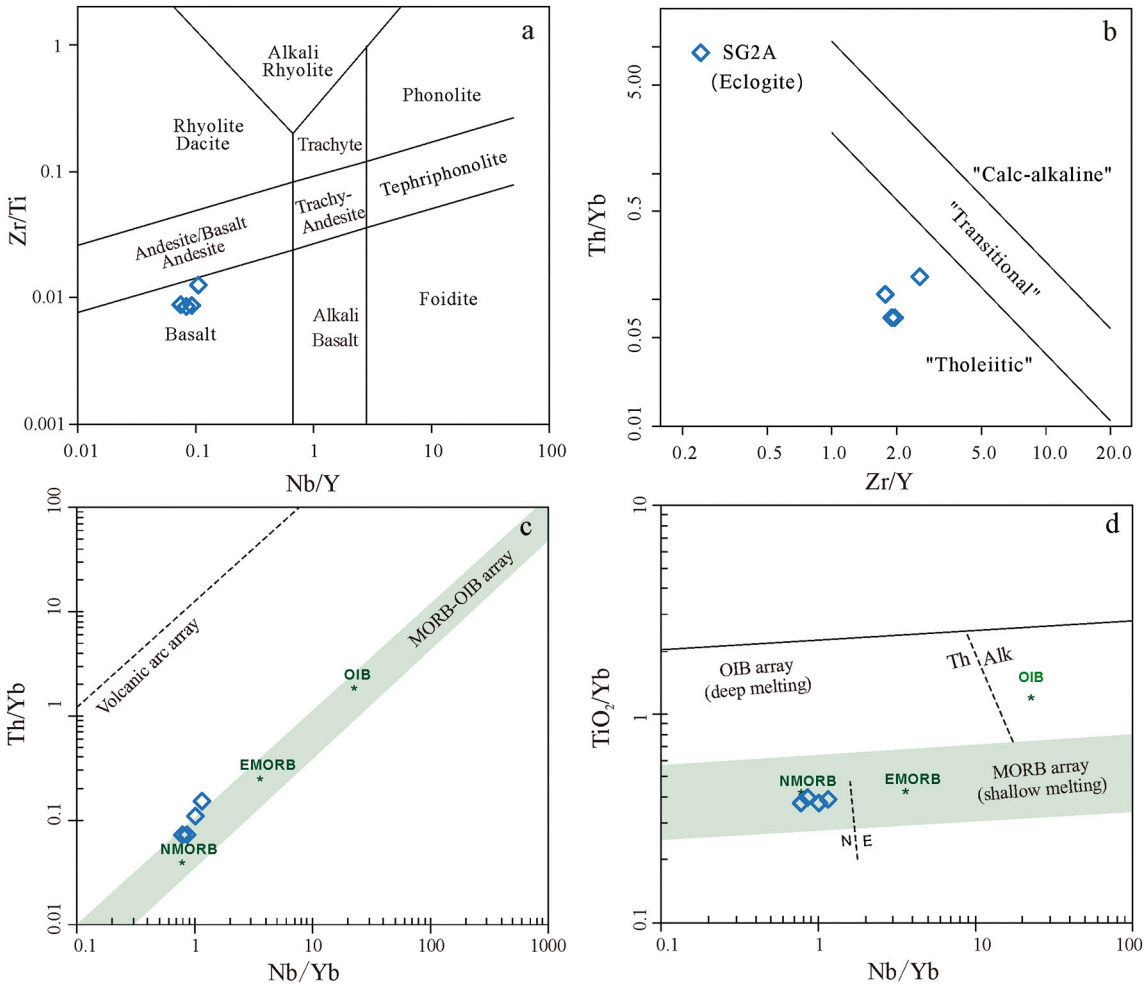

Fig. 8. Classification diagrams (a and b) and tectonic discrimination diagrams (c and d) for eclogites from the Sieggraben Complex. (a) Zr/Ti vs. Nb/Y (after Pearce, 1996), (b)Th/Yb vs. Zr/Y (after Ross and Bédard, 2009), (c) Nb/Yb vs. Th/Yb and (d) Nb/Yb vs. TiO_2/Yb (after Pearce, 2008). Abbreviations: Alk – alkaline; Th – tholeiitic; OIB – ocean island basalt; *E*-MORB and N-MORB – enriched and normal mid ocean ridge basalt.

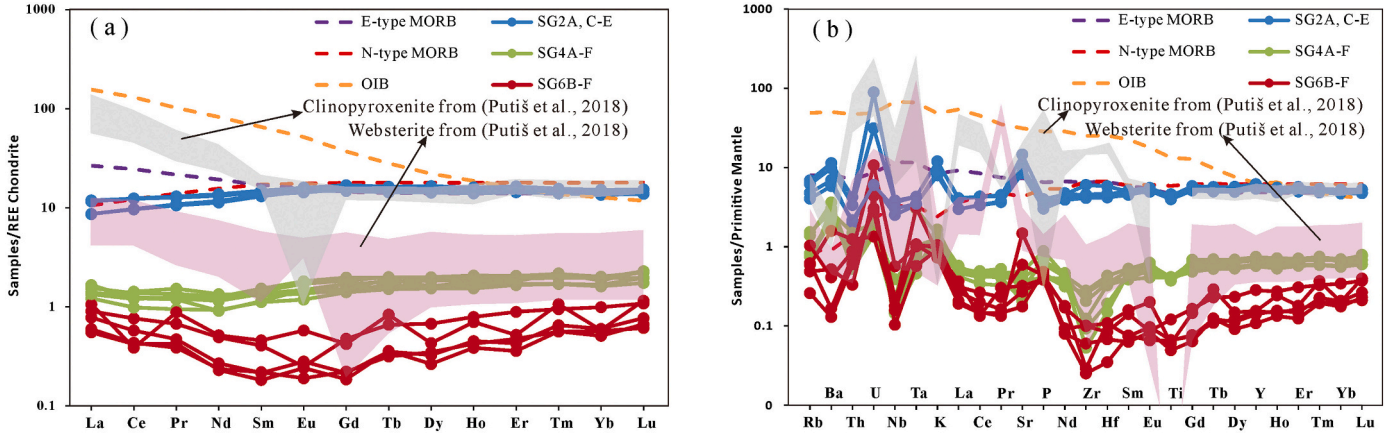

Fig. 9. Chondrite-normalized REE patterns (a) and primitive-mantle-normalized trace element (b) diagrams for eclogite and ultramafic rocks from the Sieggraben Complex of the Schäffern and Steinbach klippens. The values of chondrite and primitive mantle are from Boynton (1984) and Sun and McDonough (1989), respectively. The data of light grey and pink shaded background are from Putiš et al. (2018). (For interpretation of the references to colour in this figure legend, the reader is referred to the web version of this article.)

In summary, the single inherited age (363 Ma) represents an inherited age and is, i.e., derived from a granitoid/sedimentary source, suggests that Variscan materials existed in the Sieggraben Complex during ascent of the mantle-derived basalt. The main group with Triassic ages is considered as the protolith age of the eclogite, shows the eclogite crystallized from a tholeiitic basalt liquid and formed in Middle Triassic times. The Variscan grain was incorporated during ascent of the magma. The younger two ages (86 and 113 Ma) represent the later Cretaceous

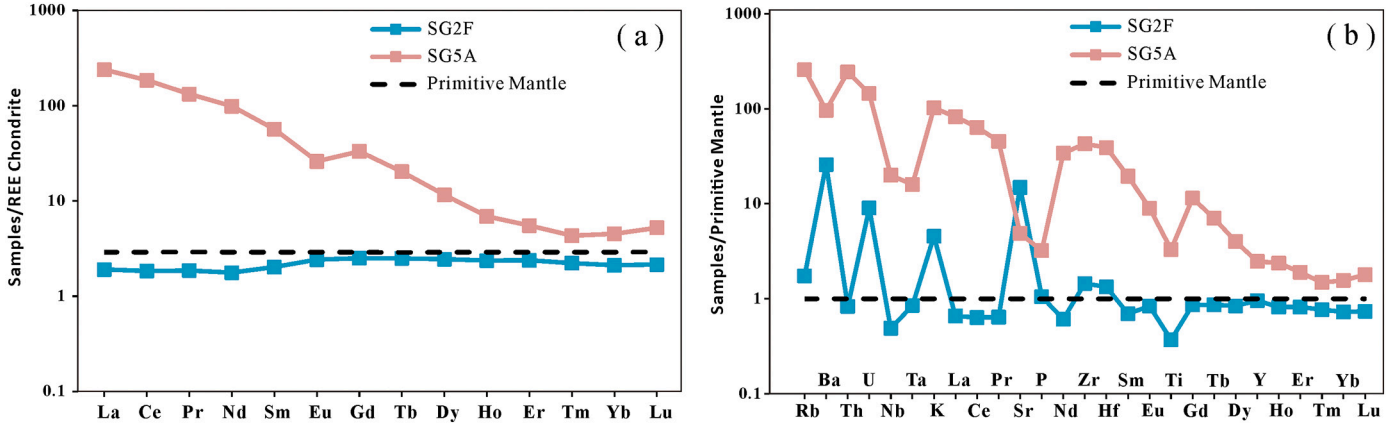

Fig. 10. Chondrite-normalized REE patterns (a) and primitive-mantle-normalized trace element (b) diagrams of trondhjemite (SG2F) and paragneiss (SG5A) from the Sieggraben Complex. The values of chondrite and primitive mantle are from Boynton (1984) and Sun and McDonough (1989), respectively.

HP metamorphic event. Up to now, only Permian Sm-Nd ages from metagabbroic eclogite protoliths from the Koralpe region were available (Thöni and Jagoutz, 1992) as mentioned above. Unmetamorphic gabbros were reported from the Eisenkappel region (Miller et al., 2011) and metagabbros with a low-grade metamorphic overprint from the Lower Austroalpine Raabalpen Complex, where these are associated to the porphyric augen-gneiss (Grobgneiss) (Schuster et al., 2001) of Permian age (Yuan et al., 2020). However, the protolith of the Sieggraben eclogite represents a tholeiitic-basaltic melt and cannot be related to the gabbro bodies mentioned before. The undated basaltic eclogites of the Kor- and Saualpe region further east show similar N-MORB characteristics as the dated Sieggraben eclogite (Miller et al., 2007). In the Kor- and Saualpe region, only two metagabbros with ages of 275 to 254 Ma (Permian) are known (Thöni and Jagoutz, 1992) and are interpreted as cumulates (Miller et al., 2007).

In Western Capathians, two Meliata units are distinguished (1) the Bôrka Nappe subducted, metamorphosed at HP–MP/LT conditions (mainly blueschist facies), and (2) Meliata s. str., metamorphosed at very-grade metamorphic conditions, a Late Jurassic–Early Cretaceous mélange containing Triassic sedimentary olistoliths (Putiš et al., 2019 and references therein). The latter unit is also found in the Eastern Alps at the Florianikogel (Fig. 1a). Recently, Putiš et al. (2019) reported U-Pb zircon ages ranging from 266 ± 3 Ma to 245.5 ± 3.3 Ma (Middle Permian to Anisian) of basalts from various blocks tectonically embedded within the Meliaticum of Western Carpathians, all with N-MORB characteristics.

The younger basalts are associated with deep-sea sediments (radiolarites). These data constrain synchronous processes and potentially tectonic relationships between the continental Sieggraben Complex in Eastern Alps and the ongoing oceanic Meliata unit of Western Carpathians although both units occur in different tectonic levels of Eastern Alps. Blocks of alkaline gabbros and diorites with cooling ages at the Permian/Triassic boundary were found in the uppermost Permian evaporite mélange (Haselgebirge) at the stratigraphic base of the Northern Calcareous Alps (Schorn et al., 2013), which is like evaporite mélanges involving Meliata basaltic blueschists in Western Carpathians (Kozur, 1991).

We consider ages of 86 Ma and 113 Ma as metamorphic ages, based on their patchy appearance in CL images and the low Th/U ratios. The older age is like the $^{40}Ar/^{39}Ar$ amphibole age from the same outcrop (Neubauer et al., 1999), but a small amount of extraneous argon in the amphibole cannot be fully excluded. The younger age of 86 ± 4 Ma is within error the same with the recently reported Lu-Hf garnet age of 89.89 ± 0.37 Ma from the Sieggraben klippe (Miladinova et al., 2021) and appears, within error, the same as that of the trondhjemite, which crosscuts the mylonitic eclogite foliation.

For the Jaklovce metabasalt of Western Carpathians, Putiš et al. (2018) reported a rutile U-Pb SIMS age of 100 ± 10 Ma (late Early Cretaceous), which is close to high-pressure age of the Sieggraben Unit.

6.1.2. *Partial melting of eclogite and formation of trondhjemite*

In the field, the trondhjemite dikes transect the foliation of eclogites, and are, therefore, younger than the peak conditions of eclogite metamorphism. The zircon grains from the trondhjemite show xenomorphic irregular habits, mostly no sign of overgrowth or zoning, only one grain has a blurry oscillatory zoning. They are significantly different from the zircon morphology in the host eclogite. These characteristics suggest that the zircons in the trondhjemite dike were not captured from the eclogite, but grew and crystallized during the formation of the dike (Vavra et al., 1996). We interpret the $^{206}Pb/^{238}U$ mean age of 82.19 ± 0.40 Ma as the best estimate for the timing of the trondhjemite dike emplacement. The zircons from the trondhjemite dike have high HREE and U contents, however, very low Th and therefore a low Th/U ratio, showing that the dike-forming magma has a good ability to dissolve and carry HREE and HFSE. This further indicates that zircons grew from a melt (Hermann et al., 2006; Liu et al., 2014; Vavra et al., 1996). These zircons show LREE depletion and HREE enrichment, which is consistent with the REE partitioning patterns of the zircons from the eclogite and other felsic magmatic rocks (Hermann et al., 2013). Compared to zircons formed within amphibolite facies metamorphic conditions we have higher HREE contents and steeper REE patterns (Rubatto, 2017). The trondhjemite and paragneiss show a completely different geochemical character (Fig. 10). Hence, we consider that the hydrous melt formed by partial melting of the eclogite during the retrograde decompressional exhumation stage. The deeply buried and subducted continental crust of the Sieggraben Complex underwent isothermal decompression during the re-entrant process, leading to decompressional hydration of the minerals in the eclogite, e.g., amphibole (for details of the eclogite retrogression path, see Neubauer et al., 1999) and/or release of structural hydroxyl groups and molecular water preserved in nominally anhydrous minerals, resulting in retrograde metamorphism of eclogite (Auzanneau et al., 2006). It also causes partial melting of the exhuming slab to produce an aqueous melt, and the trondhjemite dike might have formed by crystallization of the aqueous melt (Hermann et al., 2013; Zheng et al., 2007). The formation of melt could effectively reduce the viscosity of continental crust rocks and promote the internal disassembly of the subducted slab. Meanwhile, the aqueous melt can also function as a lubricant for the re-entry of UHP/HP rocks (Hermann et al., 2013; Labrousse et al., 2011), thus triggering or accelerating the re-entry of subducted slabs. Except a recently reported example from eclogite of the Saualpe (Schorn et al., 2021), the dated trondhjemite is the first reported magmatic rock related to the Cretaceous subduction zone and the first

Cretaceous-aged plutonic rock of the Austroalpine mega-unit. Thöni and Miller (2010) described andalusite during exhumation of the Eclogite-Gneiss Unit of the Saualpe region and this locality is also associated with small undated felsic magmatic rocks.

6.1.3. Protoliths of ultramafic rocks

Two hypotheses for the origin of ultramafic rocks proposed: (1) they are residual mantle peridotites, or (2) they are igneous cumulates, formed either by crystal fractionation or by reaction of fractionating melt with peridotite (Liu et al., 2008). In the case of Steinbach, the harzburgite-type ultramafic rocks of subcontinental *Re*-Os isotopic characteristics (Meisel et al., 1997) are intruded by the Permian clinopyroxenite dike (Putiš et al., 2018). In the two studied ultramafic rock types, the high degree of serpentinization is represented by the high LOI suggesting sea floor metamorphism conditions or metamorphic serpentinization in a subducting or exhuming slab. Trace and major-element compositions of the ultramafic rocks have LOI-corrected SiO_2 contents of 44.5 to 47.5 wt% and low $(La/Lu)_N$, $(La/Yb)_N$ ratios and Mg# between 85 and 88, as well as high Ni (1443–1970 μg/g) contents that match those expected for mantle rocks (e.g., 1883 μg/g; Workman and Hart, 2005) and lithospheric mantle peridotites (Bodinier and Godard, 2003; McDonough, 1990). Except the REE characters, the studied ultramafic rocks have a similar content of TiO_2 as websterites reported by Putiš et al. (2018). They have a different source than the eclogites (Fig. 9).

Putiš et al. (2018) reported a U-Pb zircon age of 252 ± 2 Ma (Permian/Triassic boundary) of a pyroxenite. Based on the Re isotopic composition of the Steinbach ultramafic body, Meisel et al. (1997) proposed a subcontinental mantle lithosphere for the origin of ultramafic rocks. Interestingly, ultramafic rocks are also associated with the Meliata Unit in Western Carpathians. There, perovskite formed during hydration of these rocks by a short-lived rodingitization event, and perovskite was dated within 137 and 134 Ma by the U-Pb SIMS Method (Li et al., 2014) postdating the blueschist metamorphism at 150–160 Ma, an event not reported up to now in the Sieggraben Complex.

6.1.4. History of the paragneiss

The youngest age of 262.0 ± 6.9 Ma (Fig. 6e) of typical magmatic subhedral zircons are found in broad rims of zircons and show an oscillatory zoning. These rims could have been grown in-situ during the partial melting of the paragneiss or within thin leucosome layers. This indicates that the sedimentary source is not younger than Late Permian. The youngest subcordant detrital zircon grain has an age of 493 ± 13 Ma indicating that the maximum depositional age of the paragneiss is Early Ordovician. The dominant Ediacaran age population at 597 ± 8 Ma indicate a Panafrican/Cadomian provenance as other metasedimentary units of the Eastern Alps (Siegesmund et al., 2021; Chang et al., 2021) and supports an earlier reported multi-grain U-Pb zircon age of 603 ± 23 Ma from the Sieggraben unit (Putiš et al., 2000). The rim ages of three grains indicate Variscan (Devonian – Carboniferous) metamorphism.

The existence of a strong negative Eu anomaly in the paragneiss suggests growth of Permian zircons in the continental crust because of the higher REE contents as well as the occurrence of Ediacaran detrital zircons. Permian migmatite formation and intrusion of Permian "Grobgneis"-type porphyric metagranite at about 266–272 Ma is well-known in the underlying Raabalpen basement (Chen et al., 2020; Schuster et al., 2001; Yuan et al., 2020) interpreted as rift-related magmatism and metamorphism. Therefore, in this study we suggest that the younger magmatic zircon from paragneiss formed in the same stage during rifting, and their protoliths were derived by the recycling of older continental crust. The majority of detrital zircon grains of the paragneiss with an age of 597 ± 8 Ma proofs a Panafrican source, which is similar in age with the detrital memory of the underlying Raabalpen Complex (Chang et al., 2021).

6.2. Tectonic evolution

The petrology and geochemistry of the eclogite and ultramafic rocks contained in the Sieggraben Complex of the Eastern Alps unequivocally demonstrate their mixed mantle/crust affinity and thus provide valuable constraints to the reconstruction of the Triassic geodynamic setting in the Western Tethyan realm. The most likely situation is that the Sieggraben Complex represents various lithologies from a distal continental crust of an evolving passive margin, which include fragments of tholeiitic basalts emplaced as sills in continental crust characteristic for evolving magma-rich passive margin. The U-Pb zircon dating of the eclogite revealed the dominant (sub-)concordant population giving a weighted mean age of 243.3 ± 2.6 Ma. This age is interpreted as the protolith age of eclogites and could reflect a magma emplaced during the initial stage of opening of the Meliata Ocean, which may have been a back-arc ocean related to subduction of the Paleotethys Ocean during Middle Triassic times (Froitzheim et al., 2008; Stampfli and Borel, 2004). The preliminary chemical data from undated ultramafic magmatic rocks suggest a deep-subduction zone environment with a depleted subcontinental mantle source (Meisel et al., 1997). Putiš et al. (2018) calculated P-T conditions of 850–825 °C and 25.5–27.5 kbar for a clinopyroxenite from Steinbach, which is much higher than the P-T conditions of the eclogite between 1.4 and 1.9 Gpa and 610–750 °C (Kromel et al., 2011; Miladinova et al., 2021; Neubauer et al., 1999). We assume, therefore, that eclogite and ultramafic rocks have their origin in different levels of the subducted lithosphere.

The detrital memory of biotite-rich paragneisses suggest the old continental crust metamorphosed during Variscan times close to the margin of the Meliata basin subsequently affected by Permian metamorphism and magmatism as already proposed by Schuster et al. (2001) and Schuster and Stüwe (2008) for other Austroalpine units. In the Southalpine realm however, metamorphism and magmatism, related to the Permian extension, has already been recognized earlier, and their magmatic activity is restricted to the Lower to Middle Permian with plutonic rocks and volcanics of the Southalpine unit in the age range 275–285 Ma (Schaltegger and Brack, 2007). The Southalpine Ivrea-Verbano zone includes two major periods of emplacement of mantle magmas during Early and Middle Permian (Quick et al., 2009) and Middle-Late Triassic times (Zanetti et al., 2013). In contrast to the Austroalpine mega-unit, volcanic, subvolcanic and even classical plutonic bodies of Middle to early Late Triassic age are widespread in the cover successions of the Southalpine realm (e.g., Lustrino et al., 2019 and references therein).

The U-Pb age result of the trondhjemite dike within the eclogite indicates that the melt formed at 82 Ma, significantly younger than the peak HP metamorphic age (95–90 Ma) in the Koriden Complex further west (Miller et al., 2007; Thöni, 2006), as well as recently published Lu-Hf data of 89.89 ± 0.37 Ma from the Sieggraben klippe (Miladinova et al., 2021). The relative relationships suggest that high-pressure metamorphic rocks were affected by partial melting during the exhumation process. Two zircon grains in the eclogite show metamorphic ages with 113 Ma and 86 Ma with a ca. 17 Myr time interval, interpreted as the time between peak HP metamorphism and melting during exhumation although the interpretation of these dates would be somehow speculative. The age of eclogite metamorphism by the Lu-Hf data of 89.89 ± 0.37 Ma mentioned above (Miladinova et al., 2021). This is in support of an earlier multi-grain zircon lower intercept age of 103 ± 14 Ma (Putiš et al., 2000). The trondhjemite intrusion is followed by cooling through the Argon retention temperature of white mica (ca. 425 ± 25 °C) indicated by ages between 82 and 78 Ma (Dallmeyer et al., 1996).

The paleotectonic reconstructions in the Alps of the western Tethys (Stampfli and Borel, 2004) have shown sequential back-arc basin openings along the Eurasian margin from the Late Permian–Triassic to Early–Middle Jurassic times, due to the Paleotethys closure and Neotethys opening and widening. In the eastern Mediterranean region, this

rifting phase occurred in a scenario of slab rollback, which created the oceanic Küre, Meliata, Maliac and Pindos basins, whose life spans are within that time interval. The Meliata–Maliac oceanic basin had been separated from the Mediterranean Neotethys by a major transform fault, which evolved further north in the subduction zone (Stampfli and Borel, 2004). In this tectonic scenario, the Middle Triassic protoliths of the Sieggraben Complex developed in response of back-arc opening during oceanic subduction of the Paleotethys as proposed by Stampfli and Borel (2004) and Neubauer et al. (2022).

Based on the data and discussion above, we suggest a new model for the tectonic evolution of Sieggraben Complex from the Eastern Alps, and we use only arguments from the Eastern Alps because of potential diachronous tectonic processes in Western Carpathians (Fig. 11). Recently, Putiš et al. (2021) proposed a two-wedge model for for the Jurassic-Cretaceous tectonics of Inner Western Carpathians, which includes the Meliaticum, too, which differs from the model presented here (for details, see below).

The Austroalpine Sieggraben Complex shows a location on the continental margin during Permian rifting and the Permian zircon ages of

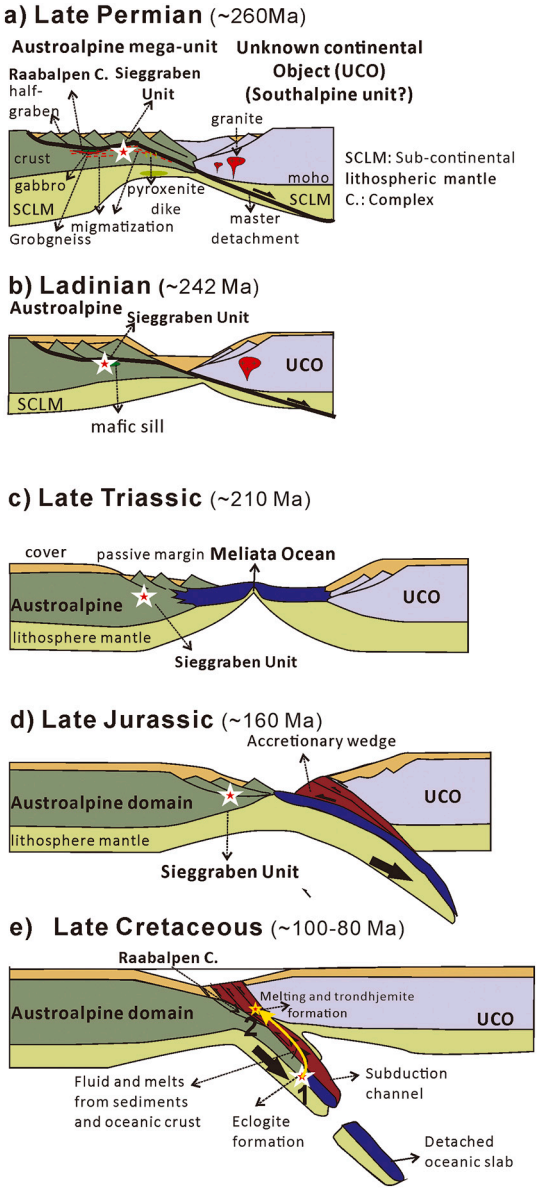

Fig. 11. Tectonic model of Sieggraben Complex and evolution of Meliata Ocean. For explanation, see text.

the dated migmatitic paragneiss indicate that process of extension. The Raabalpen Complex, now in the footwall of the Sieggraben Complex, includes Late Permian migmatites, granititic gneisses and metagabbros overlain by halfgraben-type basins filled with Permian clastic sediments and volcanics on tilted blocks (Fig. 11a) (Neubauer et al., 2022; Yuan et al., 2020). This consequently supporting the Permian rift genesis of the Austroalpine mega-unit. The Permian relationships between Austroalpine and Southalpine units are debated because of major Permian paleogeographic differences (see Neubauer et al., 2022) and Permian mega-shearing (Muttoni et al., 2019). In the model of Fig. 11a we put an "unknown continental object" (UCO). In the case that UCO was the Southalpine unit, then the widespread Southalpine magmatic rocks, particularly of the Ivrea-Verbano zone would represent, as a working hypothesis, a sort of magmatic flare-up providing the heat for migmatization. The similar age of Permian pyroxenite formation (Putiš et al., 2018) may indicate that the heat for migmatization might have been provided by ultramafic magma intrusion within the subcontinental mantle within an asymmetric rift setting (Fig. 11a). Similar Permian ultramafic rocks might be present in the Slovenska Bistrica Ultramafic Complex in the Pohorje Mountains but protolith ages are missing there (Janák et al., 2006). Middle Triassic (Ladinian) N-MOR tholeiitic-basaltic liquids intruded into the distal continental crust extended since the Permian (Fig. 11b) just predating the opening of the Meliata oceanic rift. During Middle Triassic times, the oceanic Meliata basin opened (Fig. 11c) as intially suggested by Kozur (1991). After Jurassic to Early Cretaceous consumption of the Meliata oceanic lithosphere (Fig. 11d) (Neubauer et al., 2000; Putiš et al., 2018), this piece of continental crust of the former passive margin adjacent to the Meliata oceanic lithosphere subducted during Early to early Late Cretaceous times to mantle depth (Stage 1 in Fig. 11e) as it was recently testified by Lu-Hf age of eclogitization (Miladinova et al., 2021) and also indicated by two single-grain U-Pb ages of this study. During subduction, possible Permian-Mesozoic cover successions on the Sieggraben basement were separated from their subducting basement (middle/lower crust) as postulated for other Austroalpine basement along the central axis of the Eastern Alps (e.g., Neubauer et al., 2000; Schmid et al., 2004) (Fig. 11e). The deeply buried rocks were subsequently exhumed incorporating ultramafic mantle rocks (Stage 2 in Fig. 11e). During exhumation of eclogites, partial melting took place and formation of the trondhjemite dikes during Late Cretaceous (~82 Ma). During this stage, the Sieggraben Complex was overthrusted onto the Raabalpen Complex (e.g., Dallmeyer et al., 1996).

7. Conclusions

The new data from the Sieggraben Complex combined with the literature allow the following major conclusions, and these are given here in a chronological order:

1 The host metasedimentary rocks of the Sieggraben Complex represent a distal continental crust with a Panafrican relationship, which was located close to the future margin of the Meliata basin and was affected by Permian magmatism. The host paragneisses of the Sieggraben Complex include dominant Late Ediacaran sources. The paragneiss was affected by Permian migmatization as testified by euhedral zircons with an age of 262.0 ± 6.9 Ma.
2 The ultramafic rocks were formed as part of subcontinental lithosphere and potentially by oceanic mantle lithosphere during the Permian.
3 The eclogite shows a protolith age of 242.3 ± 2.6 Ma (Anisian/Ladinian boundary) and displays a N-MORB type geochemical signature of basaltic liquids formed during Middle Triassic times. The protolith is younger than the Middle-Late Permian eclogitized metagabbros from the Koriden Complex further west.

4 After consumption and closure of the Meliata Ocean, subduction of the continental Sieggraben Complex occurred during late Early Cretaceous times and reached eclogite metamorphic conditions.
5 A trondhjemite dike cuts through the eclogite, gives a crystallization age of 82.19 ± 0.4 Ma and formed by partial melting of the host eclogite during decompression and exhumation of the previously subducted continental wedge.

Declaration of Competing Interest

The authors declare the following financial interests/personal relationships which may be considered as potential competing interests: Ruihong Chang reports financial support was provided by China Scholarship Council.

Acknowledgements

We gratefully acknowledge critical remarks and helpful suggestions by Christoph Hauzenberger, Urs Klötzli, Irena Milanidova and Marián Putiš to the initial version of the manuscript. The reviews helped to clarify content and presentation. This study was financially supported by the National Natural Science Foundation of China (grant no. 91755212), Taishan Scholars (ts20190918) and Qingdao Leading Innovation Talents (grant no. 19-3-2-19-zhc) to Yongjiang Liu and by a PhD grant of the State Scholarship Fund from the Chinese Scholarship Council (grant no. 201906170046) to Ruihong Chang.

Appendix A. Supplementary data

Supplementary data to this article can be found online at https://doi.org/10.1016/j.lithos.2022.106923.

References

Agard, P., 2021. Subduction of oceanic lithosphere in the Alps: Selective and archetypal from (slow-spreading) oceans. Earth Sci. Rev. 214, 103517.
Auzanneau, E., Vielzeuf, D., Schmidt, M.W., 2006. Experimental evidence of decompression melting during exhumation of subducted continental crust. Contr. Mineral. Petrol. 152 (2), 125–148.
Bienvenu, P., Bougault, H., Joron, J.L., Treuil, M., Dmitriev, L., 1990. MORB alteration: rare-earth element/non-rare earth hygromagmaphile element fractionation. Chem. Geol. 82, 1–14.
Bodinier, J.-L., Godard, M., 2003. Orogenic, ophiolitic, and abyssal peridotites. In: Holland, N.D., Turekian, K.K. (Eds.), Treatise on Geochemistry. Elsevier Ltd., pp. 1–73
Bouvier, A., Vervoort, J.D., Patchett, P.J., 2008. The Lu-Hf and Sm-Nd isotopic composition of CHUR: Constraints from unequilibrated chondrites and implications for the bulk composition of terrestrial planets. Earth Planet. Sci. Lett. 273 (1–2), 48–57.
Boynton, W.V., 1984. Chapter 3 - Cosmochemistry of the rare earth elements: meteorite studies. In: Henderson, P. (Ed.), Developments in Geochemistry. Elsevier, pp. 63–114.
Chang, R.H., Neubauer, F., Liu, Y.-J., Yuan, S.-H., Genser, J., Huang, Q.W., Guan, Q.-B., Yu, S.-Y., 2021. Hf isotopic constraints and detrital zircon ages for the Austroalpine basement evolution of Eastern Alps: review and new data. Earth Sci. Rev. 103772 https://doi.org/10.1016/j.earscirev.2021.103772.
Chen, Y.X., Demény, A., Schertl, H.P., Zheng, Y.F., Huang, F., Zhou, K., Jin, Q.Z., Xia, X. P., 2020. Tracing subduction zone fluids with distinct Mg isotope compositions: insights from high-pressure metasomatic rocks (leucophyllites) from the Eastern Alps. Geochim. Cosmochim. Acta 271, 154–178.
Dallmeyer, R.D., Neubauer, F., Handler, R., Fritz, H., Müller, W., Pana, D., Putiš, M., 1996. Tectonothermal evolution of the internal Alps and Carpathians: evidence from $^{40}Ar/^{39}Ar$ mineral and whole-rock data. Eclogae Geol. Helv. 89, 203–227.
Dhuime, B., Hawkesworth, C., Cawood, P., 2011. Geochemistry. When continents formed. Science 331 (6014), 154–155.
Frey, M., Desmons, J., Neubauer, F., 1999. The new metamorphic maps of the Alps: Introduction. Schweiz. Mineral. Petrogr. Mitt. 79, 1–4.
Froitzheim, N., Plašienka, D., Schuster, R., 2008. Alpine tectonics of the Alps and Western Carpathians: the Alps. In: McCann, T. (Ed.), The Geology of Central Europe, 2. Geological Society London, pp. 1141–1181.
Griffin, W.L., Wang, X., Jackson, S.E., Pearson, N.J., O'Reilly, S.Y., Xu, X.S., Zhou, X.M., 2002. Zircon chemistry and magma mixing, SE China: In-situ analysis of Hf isotopes, Tonglu and Pingtan igneous complexes. Lithos 61 (3–4), 237–269.
Griffin, W.L., Pearson, N.J., Belousova, E.A., Saeed, A., 2006. Comment: Hf-isotope heterogeneity in zircon 91500. Chem. Geol. 233 (3), 358–363.
Hermann, J., Spandler, C., Hack, A., Korsakov, A.V., 2006. Aqueous fluids and hydrous melts in high-pressure and ultra-high-pressure rocks: implications for element transfer in subduction zones. Lithos 92 (3), 399–417.
Hermann, J., Zheng, Y.F., Rubatto, D., 2013. Deep fluids in subducted continental crust. Elements 9 (4), 281–287.
Hoskin, P.W.O., Schaltegger, U., 2003. The composition of zircon and igneous and metamorphic petrogenesis. Rev. Mineral. Geochem. 53 (1), 27–62.
Hrvanović, S., Putiš, M., Bačík, P., 2014. Petrography and mineral chemistry of metaultramafics in the Austroalpine Sieggraben structural complex at Sieggraben and Schwarzenbach, Austria. Bull. Mineral-Petrol. odd. Národ. Muz. Praze 22, 105–114.
Hrvanović, S., Putiš, M., Bačík, P., 2015. Meta-harzburgites and meta-pyroxenites of the Austroalpine Sieggraben structural complex between Steinbach and Gschorrholz, Austria: an example of subducted mantle. Acta Geologica Slovaca 7, 73–84.
Jackson, S.E., Pearson, N.J., Griffin, W.L., Belousova, E.A., 2004. The application of laser ablation-inductively coupled plasma-mass spectrometry to in situ U–Pb zircon geochronology. Chem. Geol. 211 (1), 47–69.
Janák, M., Froitzheim, N., Vrabec, M., Krogh-Ravna, E.J., De Hoog, J.C.M., 2006. Ultrahigh-pressure metamorphism and exhumation of garnet peridotite in Pohorje, Eastern Alps. J. Metamorph. Geol. 24, 19–31.
Janák, M., Froitzheim, N., Yoshida, K., Sasinková, V., Nosko, M., Kobayashi, T., Hirajima, T., Vrabec, M., 2015. Diamond in metasedimentary crustal rocks from Pohorje, Eastern Alps: a window to deep continental subduction. J. Metamorph. Geol. 33, 495–512. https://doi.org/10.1111/jmg.12130.
Korikovsky, S.P., Putiš, M., Kotov, A.B., Salnikova, E.B., Kovach, V.P., 1998. High-pressure metamorphism of the phengite gneisses of the lower Austroalpine nappe complex in the Eastern Alps: mineral equilibria, P-T parameters and age. Petrology 6, 603–619.
Kozur, H., 1991. The evolution of the Meliata-Hallstatt Ocean and its significance for the early evolution of the Eastern Alps and Western Carpathians. Palaeogeogr. Palaeoclimatol. Palaeoecol. 87, 109–135.
Kromel, J., Putiš, M., Bačík, P., 2011. The Middle Austro-Alpine Sieggraben structural complex - new data on geothermobarometry. Acta Geol. Slovaca 3, 1–12.
Labrousse, L., Prouteau, G., Ganzhorn, A.C., 2011. Continental exhumation triggered by partial melting at ultrahigh pressure. Geology 39 (12), 1171–1174.
Li, X.-H., Putiš, M., Yang, X.-H., Koppa, M., Dyda, M., 2014. Accretionary wedge harzburgite serpentinization and rodingitization constrained by perovskite U/Pb SIMS age, trace elements and Sm/Nd isotopes: Case study from the Western Carpathians, Slovakia. Lithos 205, 1–14.
Li, J.-Y., Cao, S.-Y., Cheng, X.-M., Neubauer, F., Wang, H.B., Lv, M.-X., 2022. Migmatite and leucogranite in a continental-scale exhumed strike-slip shear zone: implications for tectonic evolution and initiation of shearing. GSA Bull. 134 (3–4), 658–680.
Liu, Y., Genser, J., Handler, R., Friedl, G., Neubauer, F., 2001. $^{40}Ar/^{39}Ar$ muscovite ages from the Penninic/Austroalpine plate boundary, Eastern Alps. Tectonics 20, 528–547.
Liu, Y., Zong, K., Kelemen, P.B., Gao, S., 2008. Geochemistry and magmatic history of eclogites and ultramafic rocks from the Chinese continental scientific drill hole: Subduction and ultrahigh-pressure metamorphism of lower crustal cumulates. Chem. Geol. 247 (1–2), 133–153.
Liu, X., Wu, Y., Gao, S., Wang, H., Zheng, J., Hu, Z., Zhou, L., Yang, S., 2014. Record of multiple stage channelized fluid and melt activities in deeply subducted slab from zircon U–Pb age and Hf-O isotope compositions. Geochim. Cosmochim. Acta 144, 1–24.
Ludwig, K., 2012. A Geochronological Toolkit for Microsoft Excel Berkeley Geochronology Center Sp. Pub.
Lustrino, M., Abbas, H., Agostini, S., Caggiati, M., Carminati, E., Gianolla, P., 2019. Origin of Triassic magmatism of the Southern Alps (Italy): constraints from geochemistry and Sr-Nd-Pb isotopic ratios. Gondwana Res. 75, 218–238.
Manatschal, G., 2004. New models for evolution of magma-poor rifted margins based on a review of data and concepts from West Iberia and the Alps. Int. J. Earth Sci. 93 (3).
Mandl, G.W., Ondreijikova, A., 1991. Über eine triadische Tiefasserfazies (Radiolarite, Tonschiefer) in den Nördlichen Kalkalpen - ein Vorbericht. Jahrb. Geol. Bundesanst. 134, 309–318.
McDonough, W.F., 1990. Constraints on the composition of the continental lithospheric mantle. Earth Planet. Sci. Lett. 101 (1), 1–18.
McDonough, W.F., Sun, S.S., 1995. The composition of the Earth. Chem. Geol. 120 (3–4), 223–253.
Meisel, T., Melcher, F., Tomaschek, P., Dingeldey, C., Koller, F., 1997. Re–Os isotopes in orogenic peridotite massifs in the Eastern Alps, Austria. Chem. Geol. 143, 217–229.
Miladinova, I., Froitzheim, N., Nagel, T.J., Janák, M., Fonseca, R.O.C., Sprung, P., Münker, C., 2021. Constraining the process of intracontinental subduction in the Austroalpine Nappes: implications from petrology and Lu-Hf geochronology of eclogites. J. Metamorph. Geol. https://doi.org/10.1111/jmg.12634.
Miller, C., Stosch, H.G., Hoernes, S., 1988. Geochemistry and origin of eclogites from the type locality Koralpe and Saualpe, Eastern Alps, Austria. Chem. Geol. 67, 103–118.
Miller, C., Zanetti, A., Thöni, M., Konzett, J., 2007. Eclogitisation of gabbroic rocks: Redistribution of trace elements and Zr in rutile thermometry in an Eo-Alpine subduction zone (Eastern Alps). Chem. Geol. 239 (1–2), 96–123.
Miller, C., Thöni, M., Goessler, W., Tessadri, R., 2011. Origin and age of the Eisenkappel gabbro to granite suite (Carinthia, SE Austrian Alps). Lithos 125, 434–448.
Muttoni, G., Gaetani, M., Kent, D.V., 2019. Adria as promontory of Africa and its conceptual role in the Tethys twist and Pangea A to Pangea B transformation in the Permian. Rivista Ital. Paleont. Stratigr. 125 (1), 249–269.
Neubauer, F., Dallmeyer, R.D., Takasu, A., 1999. Conditions of eclogite formation and age of retrogression within the Sieggraben unit, eastern Alps: implications for Alpine-Carpathian tectonics. Schweiz. Mineral. Petrogr. Mitt. 79, 297–307.

Neubauer, F., Genser, J., Handler, R., 2000. The Eastern Alps: result of a two-stage collision process. Mitteilungen der Österreichischen Geologischen Gesellschaft 92, 117–134.

Neubauer, F., Liu, Y.-J., Dong, Y.P., Chang, R.-H., Genser, J., Yuan, S.-H., 2022. Pre-Alpine tectonic evolution of the Eastern Alps: from Prototethys to Paleotethys. Earth Sci. Rev. 226, 103923 https://doi.org/10.1016/j.earscirev.2022.103923.

Pearce, J.A., 1996. A user's guide to basalt discrimination diagrams. Trace element geochemistry of volcanic rocks: applications for massive sulphide exploration. Geological Association of Canada, Short Course. Notes 12 (79), 113.

Pearce, J.A., 2008. Geochemical fingerprinting of oceanic basalts with applications to ophiolite classification and the search for Archean oceanic crust. Lithos 100 (1–4), 14–48.

Putiš, M., Korikovsky, S.P., Pushkarev, Y.D., 2000. Petrotectonics of an Austroalpine Eclogite-Bearing Complex (Sieggraben, Eastern Alps) and U-Pb Dating of Exhumation. Jahrb. Geol. Bundesanst. 142, 73–93.

Putiš, M., Li, X.-H., Yang, Y.-H., Li, Q.-L., Nemec, O., Ling, X.-X., Koller, F., Balen, D., 2018. Permian pyroxenite dikes in harzburgite with signatures of the mantle, subduction channel and accretionary wedge evolution (Austroalpine Unit, Eastern Alps). Lithos 314–315, 165–186.

Putiš, M., Soták, J., Li, Q.L., Ondrejka, M., Li, X.H., Hu, Z.-C., Ling, X.X., Nemec, O., Németh, Z., Ružička, P., 2019. Origin and age determination of the Neotethys Meliata Basin Ophiolite Fragments in the Late Jurassic–Early Cretaceous Accretionary Wedge Mélange (Inner Western Carpathians, Slovakia). Minerals 9, 652. https://doi.org/10.3390/min9110652.

Putiš, M., Nemec, O., Danišík, M., Jourdan, F., Soták, J., Tomek, Č., Ružička, P., Molnárová, A., 2021. Formation of a Composite Albian–Eocene Orogenic Wedge in the Inner Western Carpathians: P–T Estimates and $^{40}Ar/^{39}Ar$ Geochronology from Structural Units. Minerals 11 (988), 1–77.

Quick, J.E., Sinigoi, S., Peressini, G., Demarchi, G., Wooden, J.L., Sbisa, A., 2009. Magmatic plumbing of a large Permian caldera exposed to a depth of 25 km. Geology 37 (7), 603–606.

Ross, P.S., Bédard, J.H., 2009. Magmatic affinity of modern and ancient subalkaline volcanic rocks determined from trace-element discriminant diagrams. Can. J. Earth Sci. 46 (11), 823–839.

Rubatto, D., 2017. Zircon: the metamorphic mineral. Rev. Mineral. Geochem. 83 (1), 261–295.

Ryan, P., Dewey, J., 1997. Continental eclogites and the Wilson Cycle. J. Geol. Soc. 154 (3), 437–442.

Scambelluri, M., Rampone, E., Piccardo, G.B., 2001. Fluid and element cycling in subducted serpentinite: A trace element study of the Erro–Tobbio high-pressure ultramafites (Western Alps, NW Italy). J. Petrol. 42 (1), 55–67.

Schaltegger, U., Brack, P., 2007. Crustal-scale magmatic systems during intracontinental strike-slip tectonics: U, Pb and Hf isotopic constraints from Permian magmatic rocks of the Southern Alps. Int. J. Earth Sci. 96, 1131–1151.

Scherer, E., Munker, C., Mezger, K., 2001. Calibration of the lutetium-hafnium clock. Science 293 (5530), 683–687.

Schmid, S.M., Fügenschuh, B., Kissling, E., Schuster, R., 2004. Tectonic map and overall architecture of the Alpine orogeny. Eclogae Geol. Helv. 97, 93–117. https://doi.org/10.1007/s00015-004-1113-x.

Schnabel, W., 2002. Geologische Karte von Niederösterreich 1:200.000. Geologische Bundesanstalt, Wien.

Schorn, A., Neubauer, F., Genser, J., Bernroider, M., 2013. The Haselgebirge evaporitic mélange in central Northern Calcareous Alps (Austria): part of the Permian to lower Triassic rift of the Meliata Ocean? Tectonophysics 583, 28–48.

Schorn, S., Hartnady, M.I.H., Diener, J.F.A., Clark, C., Harris, C., 2021. H_2O-fluxed melting of eclogite during exhumation: an example from the eclogite type-locality, Eastern Alps (Austria). Lithos 390–391, 106118.

Schuster, R., Stüwe, K., 2008. Permian metamorphic event in the Alps. Geology 36 (8), 603–606.

Schuster, K., Berka, R., Draganits, E., Frank, W., Schuster, R., 2001. Lithologien, Metamorphosegeschichte und tektonischer Bau der kristallinen Einheiten am Alpenostrand. Arbeitstagung 2001, Neuberg an der Mürz 3. 7. September 2001. Geologische Bundesanstalt, Wien, pp. 29–55.

Siegesmund, S., Oriolo, S., Schulz, B., Heinrichs, T., Basei, M.A.S., Lammerer, B., 2021. The birth of the Alps: Ediacaran to Paleozoic accretionary processes and crustal growth along the northern Gondwana margin. Int. J. Earth Sci. 110, 1321–1348.

Spandler, C., Hermann, J., Arculus, R., Mavrogenes, J., 2004. Geochemical heterogeneity and element mobility in deeply subducted oceanic crust; insights from high-pressure mafic rocks from New Caledonia. Chem. Geol. 206, 21–42.

Söderlund, U., Patchett, P.J., Vervoort, J.D., Isachsen, C.E., 2004. The ^{176}Lu decay constant determined by Lu–Hf and U–Pb isotope systematics of Precambrian mafic intrusions. Earth Planet. Sci. Lett. 219 (3), 311–324.

Stampfli, G.M., Borel, G.D., 2004. The TRANSMED transects in space and time: constraints on the paleotectonic evolution of the Mediterranean domain. In: Cavazza, W., Roure, F., Spakman, W., Stampfli, G.M., Ziegler, P.A. (Eds.), The TRANSMED Atlas. The Mediterranean Region from Crust to Mantle: Geological and Geophysical Framework of the Mediterranean and the Surrounding Areas. Springer, Berlin Heidelberg, Berlin, Heidelberg, pp. 53–80.

Sun, S.S., McDonough, W.F., 1989. Chemical and isotopic systematics of oceanic basalts: implications for mantle composition and processes. Geol. Soc. Lond., Spec. Publ. 42 (1), 313–345.

Taylor, S.R., McLennan, S.M., 1985. The Continental Crust: Its Composition and Evolution. Blackwell, Oxford, pp. 1–312.

Thöni, M., 2006. Dating eclogite-facies metamorphism in the Eastern Alps – approaches, results, interpretations: a review. Mineral. Petrol. 88 (1–2), 123–148.

Thöni, M., Jagoutz, E., 1992. Some new aspects of dating eclogites in orogenic belts: Sm-Nd, Rb-Sr, and Pb-Pb isotopic results from the Austroalpine Saualpe and Koralpe type-locality (Carynthia/Styria, southeastern Austria). Geochim. Cosmochim. Acta 56, 347–368.

Thöni, M., Miller, C., 2010. Andalusite formation in a fast exhuming high-P wedge: textural, microchemical, and Sm-Nd and Rb-Sr age constraints for a Cretaceous P-T-t path at Kienberg, Saualpe (Eastern Alps). Austrian J. Geosci. 103, 118–131.

Vavra, G., Gebauer, D., Schmid, R., Compston, W., 1996. Multiple zircon growth and recrystallization during polyphase Late Carboniferous to Triassic metamorphism in granulites of the Ivrea Zone (Southern Alps): an ion microprobe (SHRIMP) study. Contrib. Mineral. Petrol. 122 (4), 337–358.

Verma, S.P., 1981. Seawater alteration effects on $^{87}Sr/^{86}Sr$, K, Rb, Cs, Ba and Sr in oceanic igneous rocks. Chem. Geol. 34 (1–2), 81–89.

Whitmarsh, R.B., Manatschal, G., Minshull, T.A., 2001. Evolution of magma-poor continental margins from rifting to seafloor spreading. Nature 413, 151–154.

Wiedenbeck, M., Allé, P., Corfu, F., Griffin, W.L., Meier, M., Oberli, F., von Quadt, A., Roddick, J.C., Spiegel, W., 1995. Three natural zircon standards for U-Th-Pb, Lu-Hf, trace element and ree analyses. Geostand. Newslett. 19 (1), 1–23.

Wiedenbeck, M., Hanchar, J.M., Peck, W.H., Sylvester, P., Valley, J., Whitehouse, M., Kronz, A., Morishita, Y., Nasdala, L., Fiebig, J., Franchi, I., Girard, J.-P., Greenwood, R.C., Hinton, R., Kita, N., Mason, P.R.D., Norman, M., Ogasawara, M., Piccoli, P.M., Rhede, D., Satoh, H., Schulz-Dobrick, B., Skår, O., Spicuzza, M., Terada, K., Tindle, A., Togashi, S., Vennemann, T., Xie, Q., Zheng, Y.F., 2004. Further characterisation of the 91500 zircon crystal. Geostand. Geoanal. Res. 28 (1), 9–39.

Workman, R.K., Hart, S.R., 2005. Major and trace element composition of the depleted MORB mantle (DMM). Earth Planet. Sci. Lett. 231 (1–2), 53–72.

Yuan, H.L., Gao, S., Dai, M.N., Zong, C.L., Günther, D., Fontaine, G.H., Liu, X.M., Diwu, C., 2008. Simultaneous determinations of U–Pb age, Hf isotopes and trace element compositions of zircon by excimer laser-ablation quadrupole and multiple-collector ICP-MS. Chem. Geol. 247 (1), 100–118.

Yuan, S.H., Neubauer, F., Liu, Y.J., Genser, J., Liu, B., Yu, S.Y., Chang, R.H., Guan, Q.B., 2020. Widespread Permian granite magmatism in lower Austroalpine units: significance for Permian rifting in the Eastern Alps. Swiss J. Geosci. 113, 18. https://doi.org/10.1186/s00015-020-00371-5.

Zanetti, A., Mazzucchelli, M., Sinigoi, S., Giovanardi, T., Peressini, G., Fanning, M., 2013. SHRIMP U–Pb Zircon Triassic Intrusion Age of the Finero Mafic Complex (Ivrea–Verbano Zone, Western Alps) and its Geodynamic Implications. J. Petrol. 54, 2235–2265.

Zheng, Y.F., Gao, T.S., Wu, Y.B., Gong, B., Liu, X.M., 2007. Fluid flow during exhumation of deeply subducted continental crust: zircon U-Pb age and O-isotope studies of a quartz vein within ultrahigh-pressure eclogite. J. Metamorph. Geol. 25 (2), 267–283.